Received: 1 June 2021 | Revised: 19 October 2021 | Accepted: 21 October 2021

DOI: 10.1111/joa.13579

Journal of Anatomy ANATOMICAL SOCIETY WILEY

ORIGINAL PAPER

Ecological correlates of the morphology of the auditory bulla in rodents: Application to the fossil record

Erica A. Scarpitti[1] | **Jonathan J. M. Calede**[1,2]

[1]School of Earth Sciences, The Ohio State University, Columbus, Ohio, USA

[2]Department of Evolution, Ecology, and Organismal Biology, The Ohio State University, Marion, Ohio, USA

Correspondence
Jonathan J. M. Calede, Department of Evolution, Ecology, and Organismal Biology, The Ohio State University, Marion, OH, USA.
Email: calede.1@osu.edu

Funding information
Ohio State University; Paleontological Society Norman Newell Early Career Award

Abstract

For rodents, hearing is essential to survival. It enables predator evasion, prey detection, and conspecific recognition; it is also likely to be constrained by the physical environment. The resulting hypothetical link between tympanic bulla morphology and ecology has never been investigated across a broad array of rodent species before. Such link may enable the determination of the ecological affinities of many fossil species only known from partial skulls. In this study, we used geometric morphometrics to quantify the shape of the auditory bulla of 197 specimens representing 91 species from 17 families of extant rodents across four different locomotory modes. We used landmarks and semi-landmarks on the ventral and lateral views of the skull to capture morphological characteristics of the bulla and external auditory meatus (EAM). Our results demonstrate an association between bullar morphology and locomotion in rodents. Bullar shape enables the correct classification of 76% of the species in our training set. Fossorial taxa, in particular, show a characteristic morphology including an asymmetric bulla with a dorsally located and laterally expanded EAM that has a small opening diameter. A phylogenetically informed flexible discriminant analysis shows a weak phylogenetic effect on tympanic morphology. There is no evidence for differences in bullar hypertrophy across locomotory categories. The application of this approach to select fossil rodents from the Oligo-Miocene shows broad agreements with prior studies and yields new locomotory inferences for 14 fossil species, including the first proposed locomotion for members of the family Florentiamyidae. Such results call for the timing of burrowing diversification in rodents to be reevaluated.

KEYWORDS
geometric morphometrics, Geomorpha, locomotion, paleoecology, tympanic bulla

1 | INTRODUCTION

The fossil record provides a fantastic laboratory to explore the effects of past climatic and environmental changes on biodiversity and morphology (Barnosky et al., 2003; Blois & Hadly, 2009; Dietl & Flessa, 2011). Rodents are of particular interest because of their high taxonomic diversity during the Cenozoic (Samuels & Hopkins, 2017); their small body size, short breeding cycles, and ecological adaptations make them helpful indicators of environmental change (Chaline, 1977). One group of rodents that is expected to closely track the environment through time is fossorial rodents (e.g., Calede et al., 2011); a group of animals whose distribution and abundance is dependent on soil and environmental characteristics (e.g., Lazo-Cancino et al., 2020; Malizia, 1998; Marcy et al., 2013). Burrowing requires numerous anatomical specializations, including auditory specializations (Becerra et al., 2013; Buffenstein, 2000; Calede et al., 2019; Chapman & Bennett, 1975; Ebensperger & Bozinovic, 2000; Francescoli, 2000; Luna & Antinuchi, 2007; Luna et al., 2002; Nevo,

1995; Piras et al., 2012; Stein, 2000; Vleck, 1979). The detection of such specializations in the fossil record would enable the identification of fossorial rodents.

The rise of burrowing species during the Oligocene is associated with increased aridification and forest loss (Samuels & Hopkins, 2017). Burrowing is a common strategy for rodents in open environments because it enables predator escape and access to new food sources (e.g., Alhajeri & Steppan, 2018). The great diversity of burrowing rodents during the Oligocene and Miocene includes several different families succeeding one another as the dominant member of the guild (Calede et al., 2011; Hopkins, 2007; Samuels & Hopkins, 2017; Samuels & Van Valkenburgh, 2009). Changes in the environment and biotic interactions between burrowing rodents likely influenced their diversity through time and the structure of modern ecosystems (Calede et al., 2011, 2019; Hopkins, 2007; Samuels & Van Valkenburgh, 2009). Assessing the diversity of burrowing rodents through time requires the determination of the locomotory ecology of numerous fossil species.

There have been considerable recent advancements in determining the locomotion of fossil rodents (Calede et al., 2019; Gobetz & Martin, 2006; Guerrero-Arenas et al., 2020; Jiménez-Hidalgo et al., 2018; Martin & Bennett, 1977; Samuels & Van Valkenburgh, 2008, 2009). These quantitative analyses have focused on the proportions of postcranial skeletons (e.g., Calede et al., 2019; Candela & Picasso, 2008; Carrizo et al., 2014; Elissamburu & de Santis, 2011; Elissamburu & Vizcaíno, 2004; Essner, 2007; Ginot et al., 2016; Lessa and Thaeler, 1989; Samuels & Van Valkenburgh, 2008) as well as the analyses of mostly complete skulls (Bertrand et al., 2016; Calede et al., 2019; Samuels & Van Valkenburgh, 2009). However, such remains are quite rare in the North American fossil record of the Oligocene and Miocene (see Calede & Glusman, 2017; Calede & Hopkins, 2012; Calede et al., 2019); this hampers the determination of locomotory modes for a large majority of fossil species. Our analysis explores a different approach that focuses on one adaptation to locomotion: hearing. Such approach requires only the preservation of the ear region of the skull, and as such, many more rodent species known only from partial crania can be incorporated into analyses.

Rodents have evolved various anatomical and physiological auditory specializations that enhance low frequency detection and enable predator evasion, prey detection, and conspecific recognition (Basso et al., 2017; Pfaff et al., 2015; Pleštilová et al., 2016; Schleich & Vassallo, 2003; Wannaprasert, 2016). In fact, the relationship between the morphology of components of the auditory apparatus, such as the middle ear ossicles, cochlea, and bony labyrinth, and ecology has been studied before in numerous species (Bhagat et al., 2020; Kerber & Sánchez-Villagra, 2018; Mason, 2001, 2016; Mason et al., 2010; Pfaff et al., 2015; Pleštilová et al., 2021). Tympanic bullar morphology itself has been investigated in specific species of mammals (Basso et al., 2017; Groves et al., 2021; Koper et al., 2021), including rodents (Alhajeri et al., 2015; Momtazi et al., 2008; Pleštilová et al., 2021; Potapova, 2019; Schleich & Vassallo, 2003; Tabatabaei Yazdi et al., 2014; Zherebtsova & Potapova, 2019) and has been shown to be associated with habitat use. In particular, inflated tympanic bullae and the associated sound amplification have been linked to open and arid environments (Alhajeri et al., 2015; Tabatabaei Yazdi et al., 2014). Other osteological correlates of the sensory system, like the orbit and its relationship with vision, have also served as proxies for locomotory studies (e.g., Smith et al., 2018). Additionally, recent work has investigated endocast morphology in relation to locomotion in rodents (Bertrand et al., 2021). Here, we build upon this work on the sensory apparatus of rodents and investigate the morphology of the external auditory bulla across a large variety of rodent species.

The objectives of our study are to investigate (1) the association between bullar morphology and locomotion in rodents and (2) use this relationship to determine the locomotory ecology of a number of extinct rodents within clades that evolved fossoriality during the Oligo-Miocene. We quantify the external morphology of the auditory bulla in both ventral and lateral views in a broad sample of extant rodents using two-dimensional geometric morphometrics, which captures shape variation across a variety of specimens. The results of our analysis of over 90 modern species of rodents support the validity of this approach. We apply it to a selection of 24 fossil species, 10 of which have existing locomotory inferences, and 14 of which do not. We provide the first locomotory inference for several fossil species, including one family (Florentiamyidae) that has no published locomotory inferences. These 14 new inferences are focused on taxa from families that evolved a burrowing ecology. By providing the first locomotory inferences for several members of the clades Sciuridae, Castoridae, Geomorpha, and Aplodontioiidea, we contribute to the data necessary for future analyses of the timing of the evolution of burrowing during the Oligo-Miocene.

2 | MATERIALS AND METHODS

2.1 | Sampling

All specimens used in the analysis were adults that were complete enough for all landmarks to be accurately placed. We used complete molar eruption associated with tooth wear and cranial suture fusions as criteria to select adult specimens. We included both males and females of extant species in our analyses when possible to account for possible sexual dimorphism in auditory bulla shape. A complete list of the specimens landmarked is provided in Table S1. Only specimens identified to the species level were used to limit the potential for possible taxonomic and ecological errors. All specimens were photographed in ventral and lateral view using either a Canon EOS Rebel SL2 or a Canon EOS Rebel T7 camera. The use of similar cameras and lenses in photographing the specimens prevents biasing from lens distortion in our analyses. Specimens were levelled to provide a consistent lateral view under the camera using clay.

We quantified the shape of the auditory bulla and external auditory meatus (EAM) in 197 specimens of modern rodents representing 91 species, 60 genera, and 17 families (Table 1). We purposefully chose a broad sample of rodents to capture much of the taxonomic

diversity and variety of body size within the order. We also paid particular attention to numerous species of extant rodents from the families represented in our fossil sample (e.g., Sciuridae, Geomyidae, and Heteromyidae). Additionally, we collected data for the tympanic bulla of 39 fossil rodent specimens representing 29 species, 18 genera, and 9 families (Table 2). This fossil sample includes a range of taxa from Oligocene and Miocene-aged deposits of North America. Half of the specimens belong to the clade Geomorpha (Flynn et al., 2008), whereas the others are primarily contemporaneous species from the families Aplodontiidae, Castoridae, Mylagaulidae, and Sciuridae; all represent groups that evolved a burrowing ecology (Calede et al., 2019; Hopkins, 2007; Samuels & Hopkins, 2017; Samuels & Van Valkenburgh, 2009). Among the 29 fossil species sampled, five were included in the training set. These are *Palaeocastor fossor*, *Palaeocastor nebrascensis*, *Palaeocastor peninsulatus*, *Entoptychus cavifrons*, and *Alphagaulus pristinus*. These five taxa were chosen because there exists a priori locomotory inferences based on postcrania for each of them (Calede, 2014; Calede & Hopkins, 2012; Calede et al., 2019; Samuels & Van Valkenburgh, 2008). We chose to include fossil taxa in the analysis to expand the range of ecomorphologies represented by the training set with morphs absent from modern faunas (i.e., burrowing beavers, an extinct clade of pocket gophers, and an entirely extinct clade of burrowers, mylagaulids).

Each of the taxa in the training set was assigned to one of four locomotory categories considered in this study: arboreal, semi-fossorial, terrestrial, and fossorial (see Table 3 for locomotion descriptions by Samuels & Van Valkenburgh, 2008). These assignments were made based on the literature (Table 1). Gliding taxa were included within the arboreal category because of the small number of species concerned. We did not sample ricochetal species because (1) they cannot be landmarked using the same approach as the other rodents we studied and (2) their locomotory ecology is less ambiguous, even when studying fossil taxa (e.g., Turnbull, 1991).

2.2 | Landmarking

We used two-dimensional geometric morphometrics to quantify variation in bullar shape across and within taxa (Table 1). Traditional landmarks (type 1) were used to represent homologous features (e.g., protocone of the third molar) and type 2 landmarks to represent geometrically equivalent points (e.g., anterior-most points of EAM). Semi-landmarks were used to quantify the curvature of the tympanic bulla and opening of the EAM (Zelditch et al., 2004). Landmarks and semi-landmarks were digitized using tpsDig 2 v.2.16 (Rohlf, 2010) with the assistance of tpsUtil v. 1.58 (Rohlf, 2013). We placed the traditional landmarks first, in the same order on each specimen. Semi-landmark curves were drawn afterwards in the same order on each specimen as well (Figures 1 and 2; Table 4). The number of semi-landmarks used in the analyses was determined by running a sensitivity analysis (see MacLeod, 1999). The analysis was run twice: once with a large number of semi-landmarks (60/30) and once with a smaller number of semi-landmarks (29/15). The goal of the sensitivity analysis was to minimize the number of semi-landmarks and the number of significant axes in the principal component analysis (see below) and maximize the percentage of variation in the dataset represented by the axes and the percentage of specimens correctly identified by the canonical variate analyses (see below). In both lateral and ventral views, the larger number of semi-landmarks proved to be optimal. We used the same landmarking scheme (semi-landmarks and landmarks) in both extant and fossil specimens. Each set of landmarks and semi-landmarks was size-calibrated using the scale included in the specimen photos in tpsDig. The centroid sizes are provided in Table S2.

2.3 | Analyses

We imported our TPS file into R. v. 4.0 (R Core Team, 2019) using Rstudio v. 1.2.5033 (RStudio Team, 2019) and the package geomorph v. 2.1.7-1 (Adams & Otárola-Castillo, 2013). The landmarks were aligned using generalized Procrustes Superimposition (Rohlf & Slice, 1990). We then used principal component analyses (PCAs) to look at similarities and differences in bullar shape for both ventral and lateral view. All specimens were included in these analyses. The scores were then averaged for each species. The species averages were used in jackknifed canonical variate analyses (CVAs; Strauss, 2010) to determine how reliably each species in the training set can be assigned to their a priori locomotion based on bulla morphology in each view. In all analyses, we only used principal component (PC) axes that explained a large amount of the morphological variation in the dataset; we made this determination using a scree plot. We also combined the PC scores for all species from both the analyses of the lateral and ventral views. This combined dataset was used to infer fossil locomotory ecology based on both aspects of bullar morphology. These data are provided in Table S3.

Because evolutionary history can have substantial impacts on morphology and species may be more similar (or dissimilar) based on shared ancestry, instead of shared ecology, we also ran a phylogenetically informed flexible discriminant function analysis (pFDA) (Schmitz & Motani, 2011). We calculated Pagel's lambda to estimate the importance of phylogeny using the phylo.fda.R script published by Schmitz and Motani (2011) and updated by Verde Arregoitia et al. (2017). A lambda value of zero represents the absence of phylogenetic signal or data consistent with a star phylogeny, whereas a lambda of one represents data consistent with the selected phylogeny under a Brownian motion model. The pFDA was run on a random sample of 100 time-calibrated trees of rodents selected from the 1000 developed by Price and Hopkins (2015) based on the Fabre et al. (2012) tree. We pruned each of the 100 trees to retain only the species for which we have morphological data. Finally, we randomly resolved all polytomies. All of the tree manipulations were performed using the packages ape (Paradis and Schliep, 2018) and mda (Hastie et al., 2009).

In addition to determining differences in bullar shape across locomotory categories, we investigated whether or not there are

TABLE 1 Extant species included in our analyses with their assigned locomotion based on the literature

ID	Family	Genus	Species	*N*	Locomotion	References
1	Anomaluridae	*Anomalurus*	*beecrofti*	4	Arboreal	Calede et al. (2019)
2	Sciuridae	*Aeretes*	*melanopterus*	1	Arboreal	Calede et al. (2019)
3	Capromyidae	*Capromys*	*pilorides*	3	Arboreal	Calede et al. (2019)
4	Erethizontidae	*Coendou*	*prehensilis*	2	Arboreal	Calede et al. (2019)
5	Erethizontidae	*Erethizon*	*dorsata*	4	Arboreal	Calede et al. (2019)
6	Sciuridae	*Glaucomys*	*volans*	2	Arboreal	Calede et al. (2019)
7	Sciuridae	*Hylopetes*	*spadiceus*	1	Arboreal	Rasmussen and Thorington (2008)
8	Anomaluridae	*Idiurus*	*macrotis*	1	Arboreal	Calede et al. (2019)
9	Sciuridae	*Paraxerus*	*cepapi*	1	Arboreal	Calede et al. (2019)
10	Sciuridae	*Petinomys*	*crinitus*	1	Arboreal	Jackson (1999)
11	Sciuridae	*Petinomys*	*lugens*	1	Arboreal	Jackson (1999)
12	Sciuridae	*Petaurista*	*petaurista*	4	Arboreal	Calede et al. (2019)
13	Sciuridae	*Pteromys*	*volans*	1	Arboreal	Calede et al. (2019)
14	Sciuridae	*Ratufa*	*bicolor*	3	Arboreal	Calede et al. (2019)
15	Sciuridae	*Sciurus*	*aberti*	1	Arboreal	Calede et al. (2019)
16	Sciuridae	*Sciurus*	*carolinensis*	3	Arboreal	Calede et al. (2019)
17	Erethizontidae	*Sphiggurus*	*mexicanus*	1	Arboreal	Calede et al. (2019)
18	Sciuridae	*Sciurus*	*niger*	1	Arboreal	Calede et al. (2019)
19	Sciuridae	*Tamiasciurus*	*douglasii*	2	Arboreal	Ransome and Sullivan (2004)
20	Sciuridae	*Tamiasciurus*	*hudsonicus*	4	Arboreal	Calede et al. (2019)
22	Aplodontiidae	*Aplodontia*	*rufa*	2	Fossorial	Calede et al. (2019)
23	Geomyidae	*Cratogeomys*	*castanops*	2	Fossorial	Calede et al. (2019)
24	Geomyidae	*Cratogeomys*	*fumosus*	4	Fossorial	Calede et al. (2019)
26	Geomyidae	*Geomys*	*arenarius*	1	Fossorial	Lessa and Thaeler (1989)
27	Geomyidae	*Geomys*	*bursarius*	1	Fossorial	Calede et al. (2019)
28	Geomyidae	*Geomys*	*personatus*	3	Fossorial	Lessa and Thaeler (1989)
29	Geomyidae	*Heterogeomys*	*heterodus*	5	Fossorial	Stein (1993)
30	Geomyidae	*Heterogeomys*	*hispidus*	1	Fossorial	Stein (1993)
31	Geomyidae	*Pappogeomys*	*bulleri*	3	Fossorial	Calede et al. (2019)
32	Spalacidae	*Rhizomys*	*sumatrensis*	1	Fossorial	Calede et al. (2019)
33	Geomyidae	*Thomomys*	*bottae*	1	Fossorial	Calede et al. (2019)
34	Geomyidae	*Thomomys*	*monticola*	3	Fossorial	Marcy et al. (2016)
35	Geomyidae	*Thomomys*	*talpoides*	2	Fossorial	Calede et al. (2019)
36	Geomyidae	*Zygogeomys*	*trichopus*	1	Fossorial	Calede et al. (2019)
37	Sciuridae	*Ammospermophilus*	*leucurus*	3	Semi-fossorial	Calede et al. (2019)
38	Cricetidae	*Arvicola*	*terrestris*	1	Semi-fossorial	Calede et al. (2019)
39	Heteromyidae	*Chaetodipus*	*baileyi*	6	Semi-fossorial	Kinlaw (1999)
40	Heteromyidae	*Chaetodipus*	*hispidus*	3	Semi-fossorial	Kinlaw (1999)
41	Heteromyidae	*Chaetodipus*	*intermedius*	2	Semi-fossorial	Verde Arregoitia et al. (2017)
42	Sciuridae	*Callospermophilus*	*lateralis*	3	Semi-fossorial	Revsbech et al. (2013)
43	Sciuridae	*Cynomys*	*leucurus*	5	Semi-fossorial	Calede et al. (2019)
44	Sciuridae	*Cynomys*	*ludovicianus*	2	Semi-fossorial	Calede et al. (2019)
45	Heteromyidae	*Chaetodipus*	*penicillatus*	3	Semi-fossorial	Verde Arregoitia et al. (2017)
46	Cricetidae	*Dicrostonyx*	*groenlandicus*	2	Semi-fossorial	Calede et al. (2019)
47	Hystricidae	*Hystrix*	*cristata*	2	Semi-fossorial	Calede et al. (2019)
48	Sciuridae	*Ictidomys*	*tridecemlineatus*	4	Semi-fossorial	Tague (2020)

TABLE 1 (Continued)

ID	Family	Genus	Species	N	Locomotion	References
49	Cricetidae	*Lemmiscus*	*curtatus*	1	Semi-fossorial	Calede et al. (2019)
50	Cricetidae	*Lemmus*	*sibiricus*	2	Semi-fossorial	Kesner (1986)
51	Cricetidae	*Microtus*	*californicus*	2	Semi-fossorial	Calede et al. (2019)
52	Sciuridae	*Marmota*	*flaviventris*	2	Semi-fossorial	Calede et al. (2019)
53	Cricetidae	*Microtus*	*longicaudus*	2	Semi-fossorial	Dutt et al. (2020)
54	Sciuridae	*Marmota*	*monax*	2	Semi-fossorial	Calede et al. (2019)
55	Cricetidae	*Microtus*	*ochrogaster*	2	Semi-fossorial	Mankin and Getz (1994)
56	Cricetidae	*Microtus*	*oeconomus*	2	Semi-fossorial	Mankin and Getz (1994)
57	Cricetidae	*Neofiber*	*alleni*	3	Semi-fossorial	Calede et al. (2019)
58	Sciuridae	*Otospermophilus*	*variegatus*	1	Semi-fossorial	Matějů and Kratochvíl (2013)
59	Heteromyidae	*Perognathus*	*fasciatus*	2	Semi-fossorial	Kinlaw (1999)
61	Cricetidae	*Phenacomys*	*intermedius*	3	Semi-fossorial	Kesner (1986)
64	Sciuridae	*Spermophilus*	*elegans*	2	Semi-fossorial	Pfeifer (1982)
65	Sciuridae	*Spermophilus*	*spilosoma*	5	Semi-fossorial	Calede et al. (2019)
66	Sciuridae	*Tamias*	*amoenus*	1	Semi-fossorial	Barker and Boonstra (2005)
67	Sciuridae	*Tamias*	*minimus*	2	Semi-fossorial	Laundré (1989)
68	Sciuridae	*Tamias*	*striatus*	1	Semi-fossorial	Snyder (1982)
69	Thryonomyidae	*Thryonomys*	*swinderianus*	2	Semi-fossorial	Weisbecker and Schmid (2007)
70	Sciuridae	*Urocitellus*	*armatus*	2	Semi-fossorial	Matějů and Kratochvíl (2013)
71	Muridae	*Apodemus*	*agrarius*	1	Terrestrial	Calede et al. (2019)
72	Muridae	*Apodemus*	*flavicollis*	1	Terrestrial	Verde Arregoitia et al. (2017)
73	Muridae	*Apodemus*	*sylvaticus*	1	Terrestrial	Montgomery (1980)
74	Nesomyidae	*Cricetomys*	*gambianus*	1	Terrestrial	Dunn and Rasmussen (2007)
75	Caviidae	*Cavia*	*porcellus*	2	Terrestrial	Calede et al. (2019)
76	Dinomyidae	*Dinomys*	*branickii*	2	Terrestrial	Calede et al. (2019)
77	Dasyproctidae	*Dasyprocta*	*punctata*	2	Terrestrial	Calede et al. (2019)
78	Heteromyidae	*Heteromys*	*anomalus*	1	Terrestrial	Rood and Test (1968)
79	Heteromyidae	*Heteromys*	*gaumeri*	3	Terrestrial	Calede et al. (2019)
80	Cricetidae	*Ichthyomys*	*tweedii*	2	Terrestrial	Calede et al. (2019)
81	Chinchillidae	*Lagidium*	*peruanum*	1	Terrestrial	Ginot et al. (2016)
82	Cricetidae	*Myodes*	*gapperi*	4	Terrestrial	Brehm et al. (2020)
83	Cricetidae	*Microtus*	*montanus*	2	Terrestrial	Brehm et al. (2020)
84	Cricetidae	*Nectomys*	*apicalis*	2	Terrestrial	Calede et al. (2019)
85	Cricetidae	*Neotoma*	*cinerea*	2	Terrestrial	Calede et al. (2019)
86	Cricetidae	*Neotoma*	*mexicana*	2	Terrestrial	Verde Arregoitia et al. (2017)
87	Cricetidae	*Ochrotomys*	*nuttalli*	2	Terrestrial	Calede et al. (2019)
88	Cricetidae	*Oryzomys*	*palustris*	6	Terrestrial	Calede et al. (2019)
89	Cricetidae	*Peromyscus*	*difficilis*	1	Terrestrial	Galindo-Leal and Krebs (1997)
90	Cricetidae	*Peromyscus*	*leucopus*	2	Terrestrial	Verde Arregoitia et al. (2017)
91	Cricetidae	*Peromyscus*	*maniculatus*	2	Terrestrial	Calede et al. (2019)
92	Cricetidae	*Peromyscus*	*pectoralis*	2	Terrestrial	Verde Arregoitia et al. (2017)
93	Cricetidae	*Reithrodontomys*	*megalotis*	3	Terrestrial	Calede et al. (2019)
94	Muridae	*Rattus*	*norvegicus*	2	Terrestrial	Calede et al. (2019)
95	Cricetidae	*Rheomys*	*underwoodi*	1	Terrestrial	Calede et al. (2019)
96	Cricetidae	*Sigmodon*	*hispidus*	1	Terrestrial	Calede et al. (2019)

Abbreviation: *N*, number of specimens included.

TABLE 2 Fossil specimens included in our analyses. The following specimens were included in the training set: AMNH 65022 (*Palaeocastor fossor*, ID: 60), LACM 16005 (*Palaeocastor nebrascensis*, ID: 62), LACM CIT890 (*Palaeocastor peninsulatus*, ID: 63), UCMP 72112 (*Entoptychus cavifrons*, ID: 25), and UWBM 32664 (*Alphagaulus pristinus*, ID: 21). Repository identifications: JODA: John Day Fossil Beds National Monument; KUVP: University of Kansas Vertebrate Paleontology Collections; AMNH: American Museum of Natural History; FMNH: Field Museum of Natural History; LACM: Natural History Museum of Los Angeles County; UWBM: University of Washington Burke Museum; UCMP: University of California Museum of Paleontology; USNM: United States National Museum of Natural History, Smithsonian Institution; and UOMNH: University of Oregon Museum of Natural and Cultural History

Repository	Specimen number	Family	Genus	Species
JODA	621	Castoridae	*Capacikala*	*gradatus*
KUVP	48109	Castoridae	*Palaeocastor*	*fossor*
AMNH	65022	Castoridae	*Palaeocastor*	*fossor*
KUVP	28380	Castoridae	*Palaeocastor*	*magnus*
FMNH	1484	Castoridae	*Palaeocastor*	*magnus*
LACM	16005	Castoridae	*Palaeocastor*	*nebrascensis*
UWBM	53218	Castoridae	*Palaeocastor*	*peninsulatus*
LACM	CIT890	Castoridae	*Palaeocastor*	*peninsulatus*
FMNH	P1461	Castoridae	*Palaeocastor*	*simplicidens*
UCMP	72112	Geomyidae	*Entoptychus*	*cavifrons*
JODA	3785	Geomyidae	*Entoptychus*	*individens*
UCMP	71058	Geomyidae	*Entoptychus*	*wheelerensis*
UCMP	86264	Geomyidae	*Entoptychus*	*wheelerensis*
UCMP	65161	Geomyidae	*Entoptychus*	*wheelerensis*
UCMP	151251	Geomyidae	*Entoptychus*	*wheelerensis*
LACM	17038	Heteromyidae	*Tenudomys*	*dakotensis*
LACM	CIT618	Eomyidae	*Paradjidaumo*	*trilophus*
AMNH	103387	Florentiamyidae	*Florentiamys*	*kennethi*
AMNH	103384	Florentiamyidae	*Florentiamys*	*kingi*
AMNH	103383	Florentiamyidae	*Sanctimus*	*falkenbachi*
AMNH	103385	Florentiamyidae	*Sanctimus*	*stouti*
AMNH	12890	Geomyidae	*Gregorymys*	*curtus*
UCMP	73782	Geomyidae	*Entoptychus*	*cavifrons*
UCMP	122004	Heteromyidae	*Harrymys*	*irvini*
UCMP	71001	Geomyidae	*Entoptychus*	*individens*
UCMP	65251	Geomyidae	*Entoptychus*	*species A*
UNSM	26686	Heteromyidae	*Schizodontomys*	*amnicolus*
AMNH	129674	Heteromyidae	*Mioperognathus*	*willardi*
UCMP	31451	Aplodontiidae	*Meniscomys*	*uhtoffi*
UWBM	32664	Mylagaulidae	*Alphagaulus*	*pristinus*
UWBM	28988	Geomyidae	*Entoptychus*	*planifrons*
UCMP	56279	Heteromyidae	*Bursagnathus*	*aterosseus*
USNM	PAL256585	Sciuridae	*Cedromus*	*wilsoni*
USNM	PAL256618	Sciuridae	*Cedromus*	*wilsoni*
USNM	PAL256584	Sciuridae	*Cedromus*	*wilsoni*
UOMNH	F5171	Sciuridae	*Protosciurus*	*condoni*
JODA	7276	Sciuridae	*Protosciurus*	*rachelae*
USNM	PAL437793	Aplodontiidae	*Altasciurus*	*relictus*
AMNH	65016	Mylagaulidae	*Umbogaulus*	*monodon*

TABLE 3 Locomotion descriptions (based on Samuels & Van Valkenburgh, 2008)

Locomotory category	Definition
Arboreal (A)	Capable of and regularly seen climbing for escape, shelter, or foraging (includes scansorial species [e.g., tree squirrels and erethizontid porcupines]). Gliding locomotion included.
Semi-fossorial (SF)	Regularly digs to build burrows for shelter, but does not forage underground (e.g., ground squirrels).
Fossorial (F)	Regularly digs to build extensive burrows as shelter or for foraging underground (e.g., gophers and mole rats). Displays a predominantly subterranean existence.
Terrestrial (T)	May dig to make a burrow (but not extensively); may show saltatory behavior, rarely climbs, never glides (e.g., rats and mice).

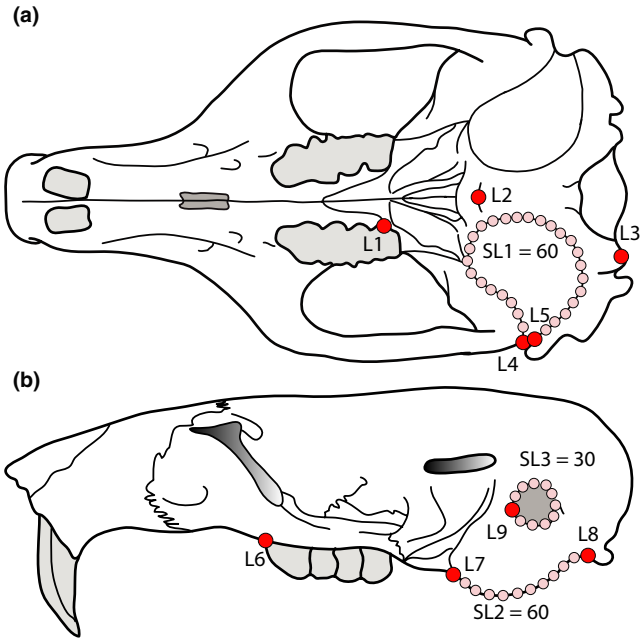

FIGURE 1 Landmarking used in our analyses. Red dots represent landmarks and pink dots represent semi-landmarks. (a) Ventral view of skull; (b) Lateral view of skull. See Table 4 for descriptions. Abbreviations: L, landmarks; SL, semi-landmarks

differences in bullar hypertrophy among locomotory categories. In ventral view, we calculated the area of the convex hull encompassing landmarks four and five as well as the curve formed by the semi-landmarks. We then calculated the ratio of this area over the total area formed by landmarks one through five. In lateral view, we calculated the area encompassed by landmarks seven and eight as well as SL2, the curve along the ventral border of the bulla. We then divided this area by the Euclidean distance between landmarks seven and eight to estimate the ventral inflation of the bulla. Areas were calculated using the package splancs 2.01-42 (Bivand et al., 2021). We compared bullar hypertrophy of rodent species across locomotory categories using a phylogenetic ANOVA for each view (ventral and lateral) to consider phylogenetic information in the variance among species (Rohlfs & Nielson, 2015). We used the simulation-base approach implemented in phytools (Revell, 2012) for this analysis. Additionally, to explore the potential role of shared ancestry in bullar size, we estimated Blomberg's *K* using picante 1.8.2 (Kembel et al., 2010) in R. A value of *K* below one indicates that closely related species resemble each other less than expected under Brownian motion trait evolution, whereas a *K* value above one indicates that closely related species are more similar than predicted by Brownian evolution.

The Procrustes superimposition process enables the rescaling of shape but does not account for the covariation of shape with size (Mitteroecker et al., 2013). To determine the possible allometric scaling of shape in our dataset, we performed a regression of the Procrustes shape coordinates on centroid size for both the ventral and lateral view datasets. We used two phylogenetically informed generalized least squares regressions (PGLS; Grafen, 1989) to evaluate the relationship between the two variables while considering the relationships between the taxa. We performed a PGLS for each of the 100 trees in our dataset, resulting in two distributions of 100 regressions, one for each view of the skull. We optimized Lambda (λ) to find the maximum likelihood transformation for each tree. The regressions were run using caper 1.0.1 (Orme et al., 2011) with code modified from Famoso et al. (2016). We used the mean of all statistics in our interpretations.

3 | RESULTS

3.1 | Principal component analyses

The PCAs show the clustering of extant species based on the morphology of their bullae (Figure 2). The PCA of the ventral view yielded six significant axes. Together, PC1 and PC2 explain 66.5% of the variation in bullar morphology in ventral view (PC1: 52.1%; PC2: 14.4%; Figure 2a). PC1 scores are associated with the extension of the EAM, whereas PC2 scores are associated with the inflation of the bulla. Locomotory categories occupy different areas of the morphospace (MANOVA: $F = 12.075$, $p < 0.0001$).

Arboreal species cluster on the negative end of the PC1 axis, which indicates a short EAM and symmetric bullae (Figure 2a). Fossorial species display positive PC1 scores associated with a laterally expanded EAM and antero-posteriorly asymmetric bullae. Semi-fossorial and terrestrial taxa range broadly along PC1 between (and overlapping with) fossorial and arboreal species. An ANOVA followed by post hoc Tukey tests (THSD) demonstrates that fossorial taxa are significantly different from all other modes of locomotion along PC1 (ANOVA: $F = 67.77$, $p < 0.0001$; THSD: $p < 0.0001$ for all three comparisons). Terrestrial taxa have the lowest scores along PC2, which are indicative of smaller auditory bullae; semi-fossorial taxa have the highest PC2 scores, which are associated with inflated

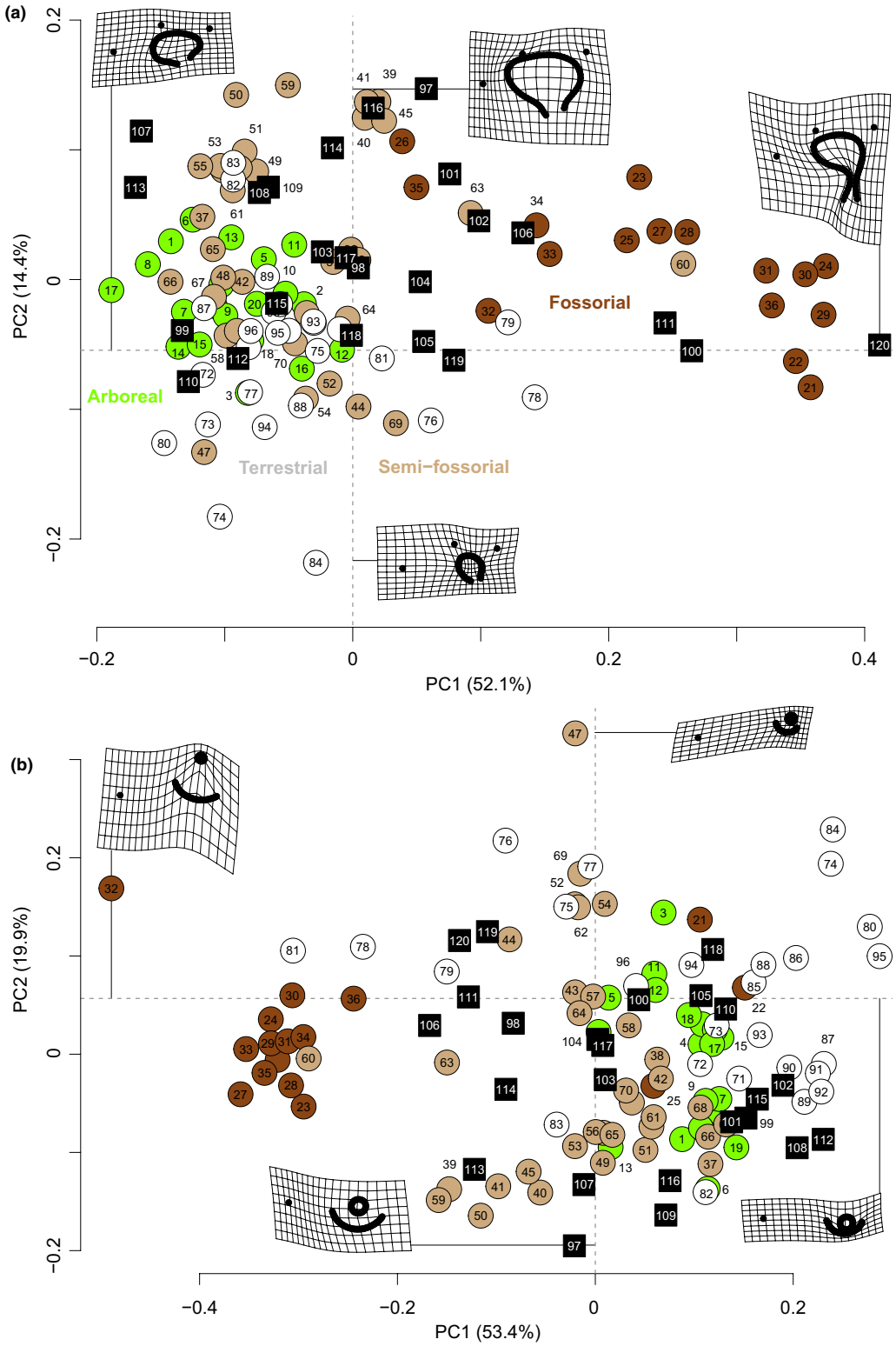

FIGURE 2 Results from the principal component analysis. (a) Ventral view; (b) Lateral view. Circles represent training-set species (see Table 1); black squares represent fossil species (see Tables 2 and 5). The deformation grids show the shape change corresponding to each axis. Numbers correspond to the identification numbers in Tables 1, 2, and 5

bullae. Arboreal and fossorial taxa occupy an intermediate position. Terrestrial taxa are significantly different from semi-fossorial and fossorial taxa along PC2 (ANOVA: $F = 9.325$, $p < 0.0001$; THSD: $p < 0.0001$ for both comparisons).

Two fossil beavers, *Capacikala gradatus* and *Palaeocastor simplicidens*, are similar in morphology to semi-fossorial taxa; *Palaeocastor magnus* is more akin to fossorial rodents. Among geomyids, *Gregorymys curtus* and *Entoptychus indet*. A, and *E. individens* are

TABLE 4 Description of the landmarks and semi-landmarks in ventral and lateral views

Ventral view	Lateral view
L1. Protocone of the third molar.	L6. Anterior-most point of the cheek teeth.
L2. Midpoint of the basioccipital at the suture with the basisphenoid.	L7. Anterior-most point of the bulla meeting the pterygoid.
L3. Posterior edge of the occipital condyle.	L8. Posterior-most point of the bulla meeting the paraoccipital process.
L4. Antero-lateral most point of the external auditory meatus.	L9. Anterior-most point of the opening of the external auditory meatus.
L5. Postero-lateral most point of the external auditory meatus.	SL2. Outlines the ventral edge of the bulla from L7 to L8 with 60 landmarks.
SL1. Outline of entire bulla from L4 to L5 with 60 semi-landmarks.	SL3. Outlines the opening of the external auditory meatus starting and ending at L9 with 30 semi-landmarks.

most similar to fossorial species. *Entoptychus planifrons* is most similar to *Palaeocastor peninsulatus*, an extinct semi-fossorial beaver; *E. wheelerensis* is also located close to semi-fossorial taxa. The three heteromyids studied, *Mioperognathus willardi*, *Schizodontomys amnicolus*, and *Bursagnathus aterosseus*, are similar in morphology to semi-fossorial taxa. *Harrymys irvini* is similar in morphology to two semi-fossorial rodents, but lies outside of the morphospace occupied by the species in the training set. *Tenudomys dakotensis*, a fossil species possibly sister taxon to Heteromyidae (Ortiz-Caballero et al., 2020), has a morphology similar to several terrestrial species and the fossorial bamboo rat *Rhizomys sumatrensis*. Among the florentiamyids included, *Florentiamys kingi* is most similar to a terrestrial taxon. *Florentiamys kennethi* is most similar to *Rhizomys sumatrensis* and the semi-fossorial *Palaeocastor nebrascensis*. *Sanctimus falkenbachi* is most similar to three semi-fossorial rodents. The morphology of *Sanctimus stouti* is most similar to *Neotoma cinerea* (terrestrial), *Petaurista petaurista* (arboreal), and *Spermophilus elegans* (semi-fossorial). The only eomyid, *Paradjidaumo trilophus*, has a bullar morphology most similar to two terrestrial mouse species. The aplodontiid *Altasciurus* has a similar morphology to many arboreal taxa but lies outside of the range of morphologies observed in the training set. Its relative, *Meniscomys uhtoffi* has a morphology most similar to semi-fossorial rodents. The one mylagaulid studied, *Umbogaulus monodon*, is most similar to fossorial taxa. In fact, it shows the most extreme morphology along PC1; it is located outside the bounds of the morphospace occupied by the training set species. It is most similar to its close relative, *Alphagaulus pristinus*, as well as extant burrowing pocket gophers. Lastly, all three sciurids included, *Cedromus wilsoni*, *Protosciurus condoni*, and *Protosciurus rachelae*, are most similar to arboreal taxa, including other arboreal squirrels.

The PCA of the lateral view yielded six significant axes. PC1 and PC2 explain 73.3% of the variance in bullar morphology (PC1: 53.4%; PC2: 19.9%; Figure 2b). PC1 scores are associated with the diameter of the EAM opening and its position relative to the ventral edge of the bulla, whereas PC2 scores are associated with the antero-posterior extension of the bulla and the diameter of the EAM opening. A MANOVA demonstrates significant differences in morphospace occupation between locomotory categories ($F = 12.29$, $p < 0.0001$).

Terrestrial species are mostly clustered at the positive end of the PC1 axis; they have antero-posteriorly small bullae and an EAM with a large opening located towards the ventral edge of the bulla. Most fossorial taxa have negative PC1 scores, indicative of an antero-posterior expanded bulla and an EAM with a small opening located at the dorsal edge of the bulla. Three fossorial species (*Aplodontia rufa*, *Alphagaulus pristinus*, and *Entoptychus cavifrons*) are located towards the positive end of PC1. Arboreal taxa are more similar to terrestrial taxa, whereas semi-fossorial taxa are located closer in morphospace to fossorial species. Post hoc tests show that fossorial taxa are significantly different from all other locomotory categories along PC1 (ANOVA: $F = 30.24$; $p < 0.0001$; THSD: $p < 0.0001$ for all comparisons). Semi-fossorial taxa are also significantly different from arboreal and terrestrial ones (THSD: $p = 0.02$ and $p = 0.004$ respectively). Along PC2, terrestrial species mostly cluster on the positive end of the axis. Semi-fossorial species are mostly located at the negative end of the axis. In fact, the two categories are the only ones that differ significantly along PC2 (ANOVA: $F = 4.288$, $p = 0.007$; THSD: $p = 0.006$). Fossorial and arboreal species overlap all other locomotory categories along this PC axis.

The fossil species studied occupy a limited range of the morphospace in the lateral view PCA. Seven occupy negative PC1 scores much smaller than zero. They range widely along PC2. A cluster of species with high PC2 values including the castorids *Palaeocastor magnus*, *Palaeocastor simplicidens*, and *Capacikala gradatus* as well as the fossil gopher *Gregorymys curtus*, the mylagaulid *Umbogaulus monodon*, and *Tenudomys dakotensis* are most similar to the terrestrial *Heteromys gaumeri* and the semi-fossorial taxa *Cynomys ludovicianus* and *Palaeocastor peninsulatus*. The other cluster, which includes *Bursagnathus aterosseus*, *Altasciurus relictus*, and *Harrymys irvini*, is near several semi-fossorial species. Two other species, *Mioperognathus willardi* and *Schizodontomys amnicolus*, have low PC2 scores; they display morphologies most similar to the terrestrial *Myodes* and the semi-fossorial *Microtus californicus*. Four taxa cluster near the origin of the morphospace: *Entoptychus indet*. A displays a morphology most similar to the terrestrial *Sigmodon* and the arboreal *Petaurista*, *Entoptychus wheelerensis* is most similar to the semi-fossorial *Urocitellus*, *Florentiamys kennethi* and *Sanctimus falkenbachi* have morphologies similar to the arboreal squirrel *Ratufa*. The two other florentiamyids, *Florentiamys kingi*, and *Sanctimus stouti* cluster near one another. *Sanctimus stouti* is most similar to the terrestrial *Rattus*, whereas *F. kingi* is most similar to the fox squirrel, *Sciurus niger*. Nearby in morphospace, *Protosciurus condoni*, a fossil sciurid displays a morphology most similar to the terrestrial mouse *Apodemus sylvaticus* and the fossorial *Aplodontia*. *Cedromus*

wilsoni clusters near the arboreal *Tamiasciurus douglassi* and the semi-fossorial *Tamias minimus*. *Protosciurus rachelae* is closest to two terrestrial taxa. The geomyid *Entoptychus planifrons* is closest in morphospace to the terrestrial *Peromyscus leucopus*; *Entoptychus individens* most resembles the semi-fossorial *Tamias minimus*. The eomyid *Paradjidaumo trilophus* displays a morphology similar to *Apodemus agrarius*. The aplodontiid *Meniscomys uhtoffi* occupies the corner of the morphospace, outside the range of morphologies occupied by species in the training set, along with *Protosciurus rachelae*. They are most similar to the terrestrial *Peromyscus difficilis*.

3.2 | Canonical variate analyses

The CVA of the ventral view yields three axes. The first two axes (Figure 3a) account for 95.9% of the variance (CV1; 70.5%, CV2: 25.4%). The four locomotory modes are well segregated in morphospace. Fossorial taxa occupy the positive end of the CV1 axis; arboreal and terrestrial taxa occupy the negative end of CV1. Arboreal taxa have positive CV2 scores, whereas terrestrial taxa have negative CV2 scores. Semi-fossorial taxa overlap with arboreal and terrestrial species and with the morphospace between these two locomotory modes and fossorial rodents. The jackknifed analysis correctly classified 69.8% of species a posteriori including 55.0% of arboreal rodents, 61.7% of semi-fossorial species, 84.6% of terrestrial taxa, and 81.3% of fossorial species. Positive CV1 scores are primarily associated with positive PC1 scores. Positive CV2 scores are associated with highly positive PC4 scores and, to a lesser extent, positive PC2, PC3, and PC5 scores, but negative PC6 scores. Therefore, species with highly positive CV1 scores have laterally expanded EAMs and asymmetric bullae, whereas species with negative CV1 scores have symmetric bullae with very short EAMs. Species with highly positive CV2 scores have round bullae with short EAMs and asymmetric bullae, whereas species with negative CV2 scores have antero-medially expanded bullae with essentially absent EAMs.

The CVA of the lateral view yields three axes. The first two axes (Figure 3b) account for 91.6% of the variance in the data (CV1; 57.3%, CV2; 34.3%). The four locomotory modes are well segregated in morphospace. Fossorial taxa occupy the negative end of CV1; arboreal and terrestrial taxa mostly occupy the positive end of the axis. Arboreal taxa have negative CV2 scores, whereas terrestrial taxa have positive CV2 scores. Semi-fossorial rodents overlap with the other three locomotory categories but occupy an intermediate location along both CV1 and CV2. The jackknifed analysis correctly classified 75% of species a posteriori including 60% of arboreal rodents, 79.4% of semi-fossorial species, 76.9% of terrestrial taxa, and 81.3% of fossorial species. Positive CV1 scores are associated with negative PC1, PC3, and PC4 scores as well as positive PC5 scores. Positive CV2 scores are mostly associated with highly positive PC4 and PC5 scores. Therefore, species with positive CV1 scores have antero-posteriorly expanded bullae with dorsally and posteriorly located EAM that have small opening diameters. Species with negative CV1 scores have antero-posteriorly short bullae with antero-ventrally located EAM that have large openings. Species with positive CV2 scores have EAMs with very large openings associated with proportionately small bullae, whereas species with negative CV2 scores have large bullae connected to EAMs with very small openings.

The combination of ventral and lateral data yields an overall correct classification rate of 75% (Figure 4a). The first two axes of this combined view CVA (Figure 4a) accounts for 91.9% of the variance in the data (CV1: 64.4%, CV2; 27.5%). The four locomotory modes are well segregated in morphospace. Fossorial taxa occupy the positive end of the CV1 axis, whereas terrestrial and arboreal species overlap on the negative end of the CV1 axis. On the CV2 axis, arboreal species occupy the negative end of the axis, whereas terrestrial species occupy the positive end of CV2. Semi-fossorial taxa cluster mostly around the intersection of the CV1 and CV2 axes. Our jackknifed CVA of the combined ventral and lateral view data correctly classified 75.0% of species a posteriori including 80% of arboreal rodents, 76.5% of semi-fossorial species, 69.2% of terrestrial taxa, and 75.0% of fossorial species. Positive CV1 scores are primarily associated with positive VPC1, VPC2, VPC6, and LPC5 scores. Positive CV2 scores are mostly associated with highly positive LPC4 and VPC6 scores but negative VPC4 scores. CV1 represents the variation from somewhat asymmetric bullae with dorsally and posteriorly located EAM that are greatly expanded laterally and have small opening diameters to more antero-posteriorly symmetric bullae that have short EAMs with large openings. CV2 represents the variation from large medially flattened auditory bullae with short, anteriorly directed EAMs that have smaller openings (negative end of the axis) to large round auditory bullae with very large openings of an extremely short posteriorly directed EAM that barely extends from the lateral edge of the tympanic cavity (positive end of the axis).

The castorid *Palaeocastor magnus* is classified as fossorial, whereas *P. simplicidens* and *Capacikala gradatus* are classified as semi-fossorial species (Table 5). The geomyids *Entoptychus individens*, *E. planifrons*, and *E. wheelerensis* are classified as semi-fossorial, whereas *Gregorymys curtus* and *Entoptychus indet*. A are classified as fossorial. The heteromyids *Schizodontomys amnicolus* and *Bursagnathus aterosseus* are classified as semi-fossorial; *Mioperognathus willardi* is classified as terrestrial (49%) although a semi-fossorial locomotion is almost as likely (46%). *Harrymys irvini* is classified as arboreal. *Tenudomys dakotensis* is classified as semi-fossorial. Three of the four florentiamyids studied, *Sanctimus stouti*, *Sanctimus falkenbachi*, and *Florentiamys kennethi*, were classified as terrestrial. The fourth one, *Florentiamys kingi* was classified as semi-fossorial. The eomyid *Paradjidaumo trilophus* was classified as terrestrial. The aplodontiid *Altasciurus relictus* was classified as arboreal, whereas its relative *Meniscomys uhtoffi* was classified as semi-fossorial. *Umbogaulus monodon* was classified as fossorial. All sciurids were found to be arboreal, but to differing degrees. *Cedromus wilsoni* was classified with a high posterior probability (94%); the classification of *Protosciurus rachelae* was associated with a lower probability (83%) and the classification of *Protosciurus condoni* is equivocal (45% arboreal; 37% semi-fossorial).

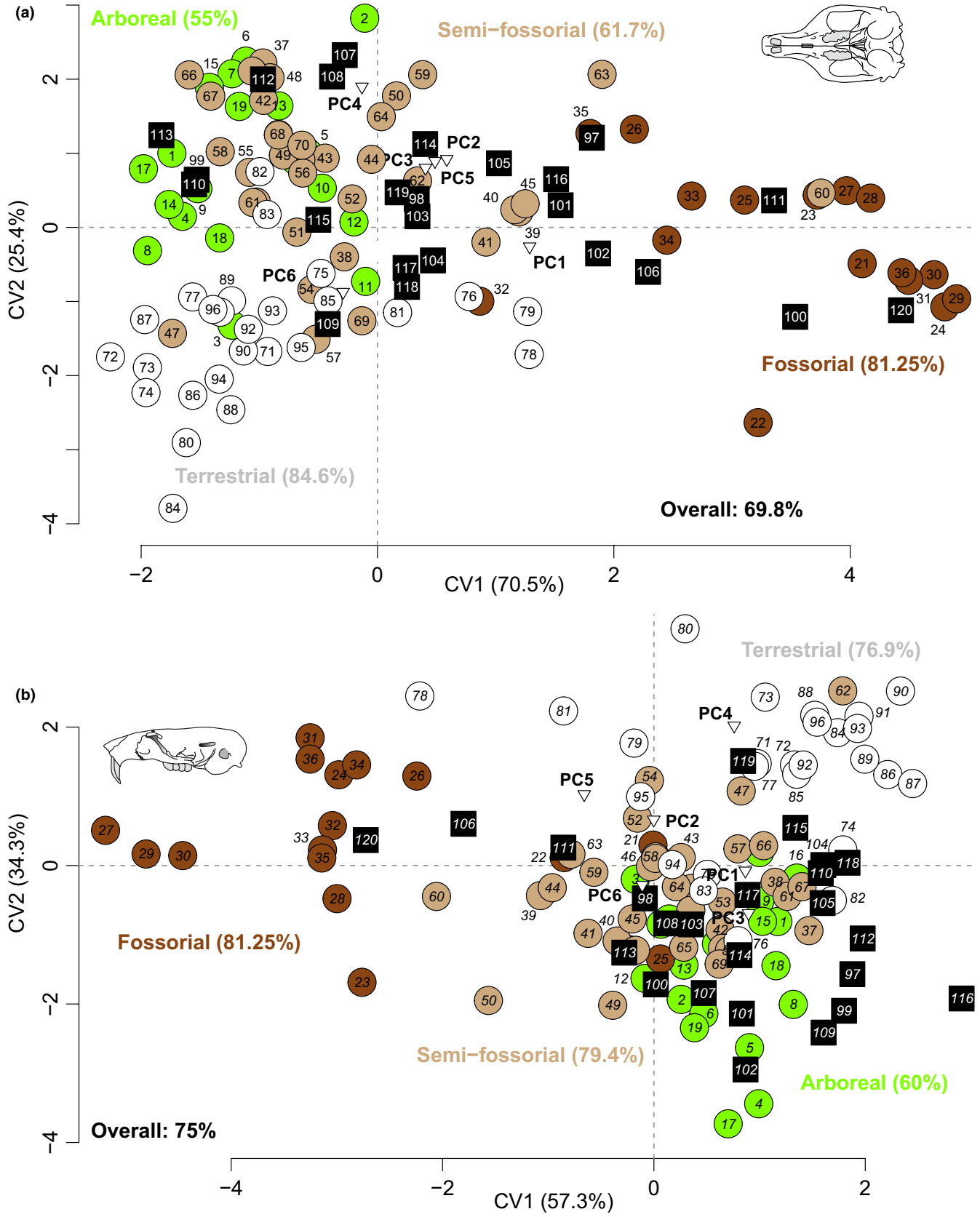

FIGURE 3 Results from the canonical variate analysis. (a) Ventral view; (b) Lateral view. Circles represent training-set species (see Table 1); black squares represent fossil species (see Tables 2 and 5). Numbers correspond to the identification numbers in Tables 1, 2, and 5. Percentages of correct a posteriori classification provided in parentheses for each locomotion and overall. Triangles show association between principal component (PC) scores and canonical variate (CV) axes

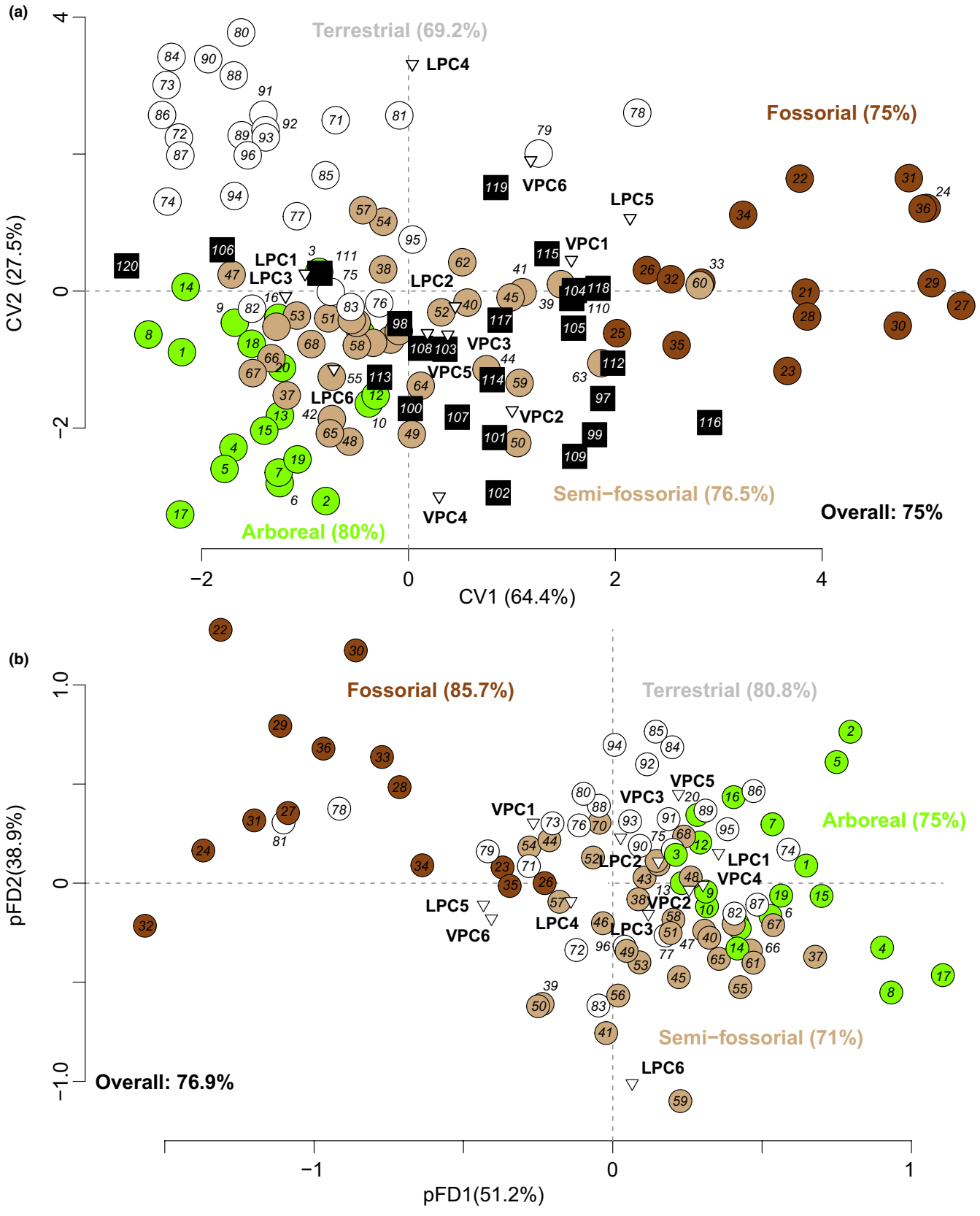

FIGURE 4 Results from the classification analyses with both views included. (a) Combined canonical variate analysis; (b) Phylogenetic flexible discriminant function analysis. Circles represent training-set species (see Table 1); black squares represent fossil species (see Tables 2 and 5). Numbers correspond to the identification numbers in Tables 1, 2, and 5. Percentages of correct a posteriori classification provided in parentheses for each locomotion and overall. Triangles show association between principal component (PC) scores (V, ventral; L, lateral) and canonical variate (CV) axes

TABLE 5 Locomotory inferences for fossil species included in our analyses (excluding those in the training set)

ID	Family	Genus	Species	Inferred locomotion	Associated probability (%)
99	Sciuridae	*Cedromus*	*wilsoni*	Arboreal	94
107	Heteromyidae	*Harrymys*	*irvini*	Arboreal	89*
110	Sciuridae	*Protosciurus*	*condoni*	Arboreal	45*
112	Sciuridae	*Protosciurus*	*rachelae*	Arboreal	83
113	Aplodontiidae	*Altasciurus*	*relictus*	Arboreal	100
97	Heteromyidae	*Bursagnathus*	*aterrosseus*	Semi-fossorial	85
98	Castoridae	*Capacikala*	*gradatus*	Semi-fossorial	75
101	Geomyidae	*Entoptychus*	*individens*	Semi-fossorial	94
102	Geomyidae	*Entoptychus*	*planifrons*	Semi-fossorial	69*
103	Geomyidae	*Entoptychus*	*wheelerensis*	Semi-fossorial	51
105	Florentiamyidae	*Florentiamys*	*kingi*	Semi-fossorial	96*
108	Aplodontiidae	*Meniscomys*	*uhtoffi*	Semi-fossorial	60
114	Castoridae	*Palaeocastor*	*simplicidens*	Semi-fossorial	95
116	Heteromyidae	*Schizodontomys*	*amnicolus*	Semi-fossorial	90*
119	Heteromyidae	*Tenudomys*	*dakotensis*	Semi-fossorial	94
104	Florentiamyidae	*Florentiamys*	*kennethi*	Terrestrial	85*
109	Heteromyidae	*Mioperognathus*	*willardi*	Terrestrial	49*
115	Eomyidae	*Paradjidaumo*	*trilophus*	Terrestrial	84*
117	Florentiamyidae	*Sanctimus*	*falkenbachi*	Terrestrial	80*
118	Florentiamyidae	*Sanctimus*	*stouti*	Terrestrial	90*
100	Geomyidae	*Entoptychus*	*indet.* A	Fossorial	90*
106	Geomyidae	*Gregorymys*	*curtus*	Fossorial	91*
111	Castoridae	*Palaeocastor*	*magnus*	Fossorial	96*
120	Mylagaulidae	*Umbogaulus*	*monodon*	Fossorial	100*

New inferences are denoted by an asterisk.

3.3 | Phylogenetic flexible discriminant function analysis

We used a pFDA to examine the relationship between bullar morphology and locomotion while accounting for the shared evolutionary history among all 91 species of extant rodents included in the analyses (Figure 4b). There is a weak effect of evolutionary ancestry on the bullar morphology of rodents (mean optimal λ over 100 trees = 0.22; standard deviation: 0.00026). The first two axes of the pFDA (Figure 4b) account for 90.1% of variation (pFD1; 51.2%, pFD2; 38.9%). The four locomotory modes are well segregated in morphospace. Fossorial taxa occupy the negative end of the pFD1 axis; arboreal taxa mostly occupy the positive end of pFD1. Most terrestrial taxa have positive pFD2 scores, whereas semi-fossorial taxa mostly occupy the negative end of the axis. They are located between arboreal and fossorial taxa along pFD1. The overall correct classification rate is 76.9% (Figure 4b). The analysis correctly classified 75.0% of arboreal species, 85.7% of fossorial species, 71.0% of semi-fossorial taxa, and 80.8% of terrestrial species. Negative pFD1 scores are associated with positive VPC1, VPC6, and LPC5 scores but negative LPC1, VPC4, and VPC2 scores. Positive pFD2 scores are mostly associated with positive VPC1, VPC3, and VPC5 scores but negative LPC6 scores.

3.4 | Bullar hypertrophy and allometry

The analysis of bullar hypertrophy (Table S4) using a phylogenetic ANOVA run across all 100 trees shows no significant differences in bullar size among locomotory categories (mean p value of 0.316 for the ventral view and 0.153 for the lateral view) (Figure 5). Our analysis of the phylogenetic signal in bullar hypertrophy leads a mean K value for the ventral view of 0.53 ($p = 0.001$ for all trees) and 0.41 for the lateral view (mean $p = 0.001$, $p < 0.05$ across all trees). For absolute bullar size, we recover a K of 1.01 in ventral view ($p = 0.001$ for all trees) and 1.0 in lateral view ($p = 0.001$ for all trees). Whether in ventral (Figure 6a) or lateral view (Figure 6b), there is no significant relationship between absolute bullar size (represented by centroid size) and morphology (as represented by PC1). The PGLS analysis of the ventral view data yields a mean p value of 0.485 and the PGLS of the lateral view data yields a mean p value of 0.231.

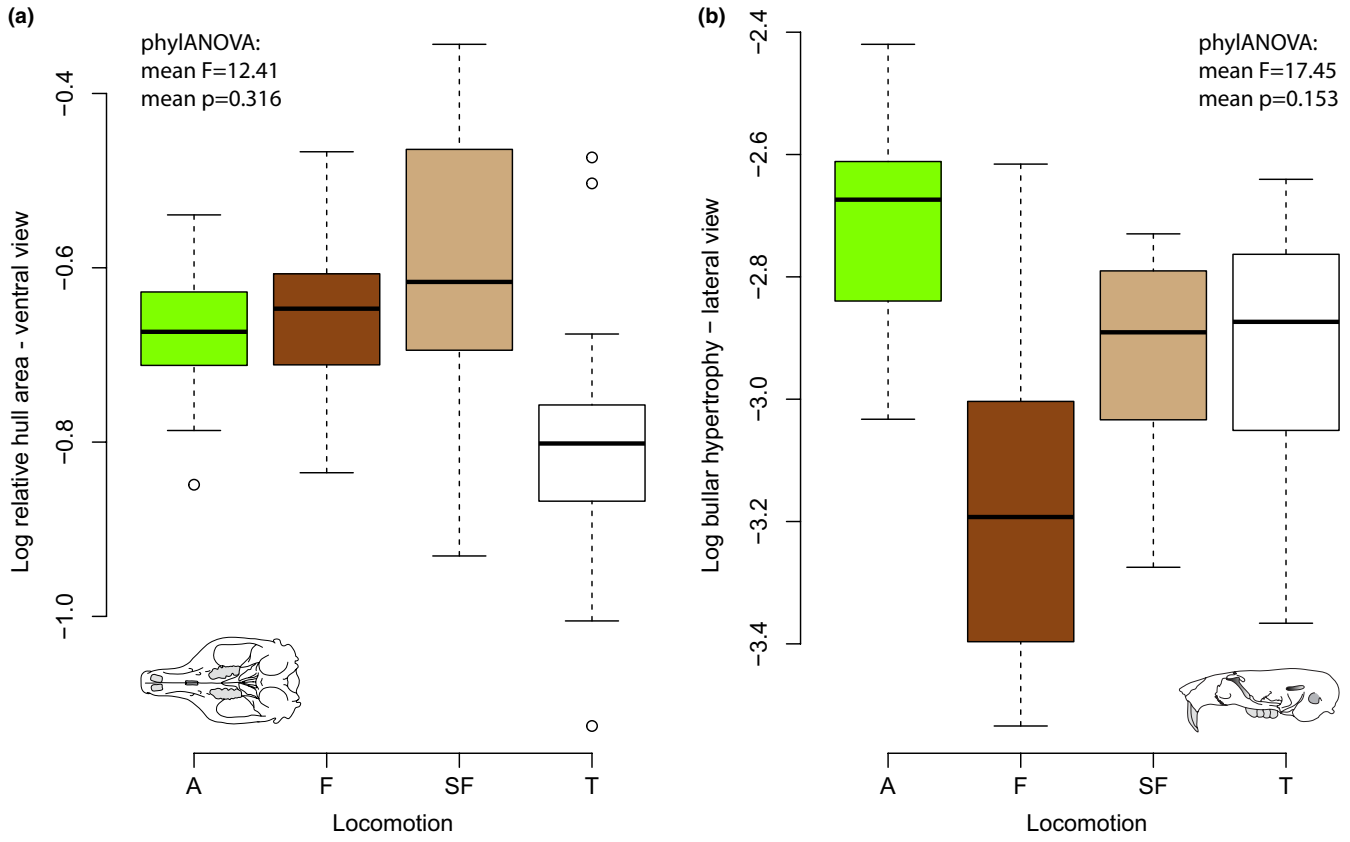

FIGURE 5 Boxplot showing variation in bullar hypertrophy. (a) Relative size of the bulla in ventral view; (b) Hypertrophy of the bulla in lateral view. Dark line in each box represents the median; open circles represent outliers. Abbreviations: A, arboreal; F, fossorial; SF, semi-fossorial; T, terrestrial

4 | DISCUSSION

The objectives of this study were to investigate (1) the association between bullar morphology and locomotion in rodents and (2) use this relationship to determine the locomotory ecology of several extinct rodents within clades that evolved fossoriality during the Oligo-Miocene. Overall, our results provide evidence that bullar morphology is indeed associated with locomotion in rodents. In fact, bullar shape alone can accurately classify the locomotion of 76% of the 96 species included in the training set. This is a very encouraging result considering the uncertainties around some natural history accounts of locomotion of some rodents as well as the inherent loss of information associated with the discretization of a taxon's locomotion into mutually exclusive categories. Prior analyses have produced locomotory inferences for rodents across a broad taxonomic range based on the morphology of complete or mostly complete skulls, including components of the auditory apparatus (Calede et al., 2019; Samuels & Van Valkenburgh, 2009). Tympanic bullar morphology itself has been investigated in select mammal species (Basso et al., 2017), including rodents (Alhajeri et al., 2015; Momtazi et al., 2008; Pleštilová et al., 2016, 2021; Schleich & Vassallo, 2003; Tabatabaei Yazdi et al., 2014). The results presented herein are the first evidence of the utility of tympanic bulla morphology in identifying locomotion across a taxonomically broad sample of rodents.

Although bullar shape is informative of locomotory ecology, we do not find evidence for an association between bullar hypertrophy and locomotion; our phylogenetic ANOVA shows no significant differences in relative bullar size across locomotory categories. Yet, past studies of the rodent tympanic apparatus have found a significant relationship between bullar size and ecology. For example, desert species within the gerbil genus *Meriones* have more hypertrophied bullae than mesic ones (Momtazi et al., 2008). Many gerbillines in fact display such a pattern (Lay, 1972). Among muroids more generally, rodents with larger tympanic bullae live in more arid and cooler environments (Alhajeri et al., 2015). There also appears to be a correlation between xeric habitat and bullar size in caviomorph rodents (Álvarez et al., 2015). A broader sampling of rodents across most extant families reveals a similar pattern in which bullar size increases with increased aridity (Alhajeri & Steppan, 2018). However, there are exceptions to this pattern. Thus, there is no evidence for a direct association between aridity and bullar size in Heteromyidae (Webster & Webster, 1975). The association between bullar size and aridity is also not verified in the burrowing genus *Ctenomys* (Francescoli et al., 2012). The association between environmental variables and bullar size is also weak in *Gerbillus* (Alhajeri & Steppan, 2018). The analysis of two species of *Tachyoryctes* failed to show bullar inflation in the more subterranean taxon (Pleštilová et al., 2021). The lack of relationship between relative bullar size and locomotion

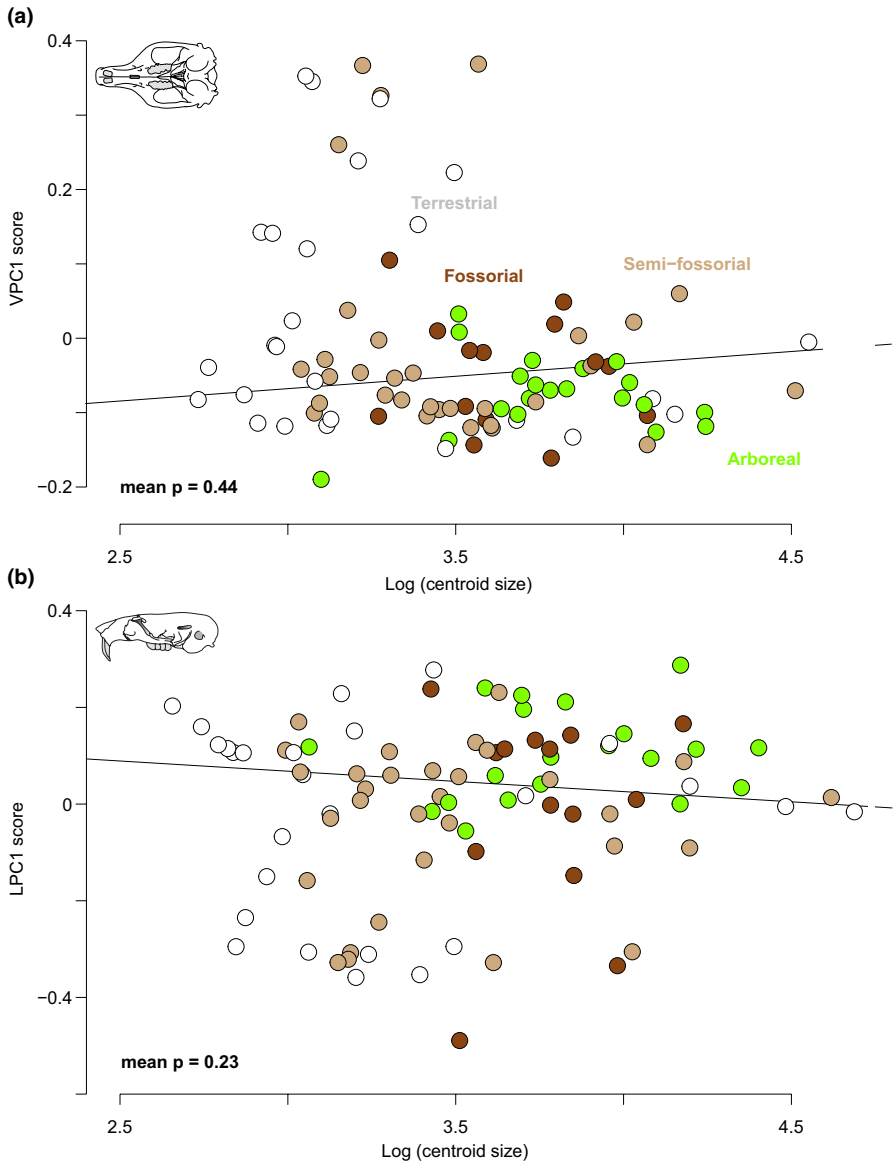

FIGURE 6 Results from the phylogenetically informed generalized least squares regressions. (a) Ventral skull; (b) Lateral skull. One of the one hundred analyses is shown for each view of the skull. The mean *p* value for each set of 100 regressions is also displayed

we find may be the consequence of several factors. First, the locomotory categories we studied encompass diverse interactions with canopy cover (Essner, 2007) and varied habitats (Hafner & Hafner, 1988; Table 1). Additionally, closely related species with similar locomotion may span a range of habitats and aridity levels (see Alhajeri & Steppan, 2018, Supplementary Data S2 for examples). Second, many of the prior analyses on bullar size and ecology focused on ricochetal taxa (e.g., Alhajeri et al., 2015; Lay, 1972; Momtazi et al., 2008; Tabatabaei Yazdi et al., 2014), which have greatly inflated bullae (relative to their non-ricochetal relatives; e.g., Hafner & Hafner, 1988) and were not included in our sample.

Burrowing rodents have poor hearing (Heffner & Heffner, 1992) but hear best at low frequencies (e.g., Begall & Burda, 2006; Heffner et al., 1994, 2001; Lange et al., 2006). Hypertrophied bullae allow for improved hearing at low frequency in open habitats where sound dissipates quickly (Alhajeri & Steppan, 2018; Francescoli et al., 2012; Webster & Webster, 1975). As a consequence, bullar hypertrophy has been associated with improved low frequency hearing, including in rodents, and particularly in burrowers (see Alhajeri & Steppan, 2018; Francescoli et al., 2012; Schleich & Vassalo, 2003). The fossorial rodents included in this study do not have significantly larger bullae than rodents in other locomotory categories. In fact, several fossorial rodent taxa do not exhibit inflated bullae despite their subterranean ecology. This includes *Heterocephalus glaber*, the naked mole rat, in which the size of the auditory bulla may be constrained as a result of the size and position of the mandible, which enables tooth-digging (Alhajeri & Steppan, 2018). The position of the jaw bones also prevents bullar inflation in another burrower, *Ctenomys* (Verzi & Olivares, 2006). The burrowing species included in our sample are dominated by geomyids, which have relatively

poor hearing (Heffner & Heffner, 1990) including at low frequencies (Wilkins et al., 1999). Although some geomyids display some bullar inflation (Wahlert, 1991), it does not seem to be directly associated with low-frequency hearing. Instead, geomyids seem to have a hearing apparatus adapted to dampening sounds in the noisy setting of the American plains (Wilkins et al., 1999). *Aplodontia*, another taxon in our dataset also has relatively poor hearing (Carraway & Verts, 1993) with a cochlea specialized for detecting slow changes in air pressure within the burrow (Merzenich et al., 1973). Our sample of fossorial rodents also includes the Spalacidae *Rhyzomys*. Another spalacid taxon, *Tachyoryctes*, does not show evidence for an association between bullar inflation and degree of burrowing (Pleštilová et al., 2021). Studies of other small mammals demonstrate that enhanced low frequency hearing can be achieved without the inflation of the auditory bulla (Heffner & Heffner, 1985). The relationship between low frequency hearing and inflated bullae in open-habitat burrowing rodents does not appear to be generalizable; we are not the first ones to identify this contradiction to the accepted paradigm (Arnaudo et al., 2020).

In addition to a lack of difference in relative bullar size across locomotory categories, we also do not find evidence for a significant influence of absolute bullar size on bullar shape (i.e., form). This suggests that within rodents, the size of the auditory apparatus evolved somewhat independently of its shape. Additionally, absolute bullar size is phylogenetically conserved ($K > 1$ for both lateral and ventral views), a consequence of the concentration of most of the larger taxa in our sample within Hystricomorpha and the presence of many of the smaller species we included within Muroidea (Table S2). Future analyses of bullar size across a broader range of rodent taxa will enable a more rigorous assessment of the co-evolution of bullar size and shape in rodents.

The bullar shape of fossorial rodents appears to be associated with hearing functionality and partially a consequence of the modifications of the cranium associated with burrowing adaptations. Fossorial rodents have a bulla that is ventrally expanded but antero-posteriorly and medio-laterally short. The bulla is asymmetric with a dorsally located and laterally expanded EAM that has a small opening diameter and is posteriorly directed. EAM length is variable among burrowing rodents (e.g., Mason et al., 2010; Verzi & Olivares, 2006); however, a laterally expanded EAM has already been identified as a characteristic of fossorial rodents (Calede et al., 2019; Verzi & Olivares, 2006). This lateral expansion of the EAM is likely a consequence of the broadening of the occipital region of the skull in burrowing rodents. Such broadening is apparent in head-lift digging rodents including Spalacidae and Mylagaulidae as well as some scratch-digging taxa like *Aplodontia* (Hopkins, 2005; Samuels & Van Valkenburgh, 2009). Even within scratch-digging and chisel-tooth digging Geomyidae (Marcy et al., 2016; Samuels & Van Valkenburgh, 2009), several taxa are characterized as platycephalic, particularly *Cratogeomys* (Russell, 1968); they have flat roofs and broad basicrania (Wilkins & Woods, 1983). Broad occiputs (that are sometimes anteriorly tilted) enable an increased area of attachment for muscles associated with packing the burrow ceiling (Hopkins, 2005). The small opening of the EAM may be associated with hearing. Occlusion of the meatus has been demonstrated to lead to better sound transmissions, particularly at low frequencies (Mason et al., 2010). It is possible that the small opening diameter of the EAM in burrowing rodents participates in improving their poor hearing.

The dorsal location of the EAM of many burrowing rodents, including geomyids, has already been recognized by Calede et al. (2019). Dorsally located EAMs are also found in some semi-aquatic rodents (Rybczynski et al., 2010) and the platypus (Manger et al., 1998). They may be associated with the position of the external ear above ground/water as well as the ability to close the meatus (Langworthy & Richter, 1938; Manger et al., 1998). The asymmetry of the bulla of burrowers is likely a consequence of the inflation of the bulla. Within geomyids (Wahlert, 1991) as well as ctenomyids (Verzi & Olivares, 2006), for example, different regions of the tympanic and mastoid may be inflated, leading to varied bullar morphology and asymmetry. Indeed, the position of the auditory bulla relative to landmarks two and three supports the conclusion that the asymmetry of the bulla of fossorial rodents is a consequence of greater inflation in the anterior portion of the tympanic as opposed to the posterior portion of the bulla with the mastoid.

Semi-fossorial rodents display round bullae (in lateral view) that are flattened anteriorly (in ventral view) with EAMs that are essentially so short that they appear absent. The short EAMs are interesting in light of their lateral expansion in fossorial taxa; semi-fossorial taxa are more similar to terrestrial ones in this aspect of bullar morphology. This hints at additional support for the fact that the length of the EAM in burrowing rodents is a consequence of the rearrangement of their skull morphology rather than an adaptation to acoustic performance (see also Mozaffari et al., 2021). The anterior flattening of the bulla in semi-fossorial taxa provides additional evidence that bullar inflation is unlikely to be uniformly associated with burrowing. The shape of the bullae is of additional interest when comparing semi-fossorial and arboreal taxa. Indeed, overall tympanic bulla shape is conserved within Sciuridae across locomotory types (Potapova, 2019). This once again shows that bullar morphology is influenced by evolutionary history. The fact that our pFDA still shows a distinction between semi-fossorial and arboreal rodents (and even sciurids) demonstrates that the shape of the anterior end of the bulla in ventral view appears to enable the distinction between semi-fossorial and arboreal taxa.

Terrestrial species have round symmetric bullae that have short anteriorly directed ventral EAMs with a large opening. The auditory bullae are small compared to other ecologies. The large opening of the EAM is a theme of the epigeic and arboreal locomotory categories. This large opening may be associated with an improved intake of auditory information into the EAM for transmission to the middle ear. Indeed, the wide unobstructed opening of the EAM is critical to hearing (Mozaffari et al., 2021) and, presumably, the identification of sounds by prey, predators, and conspecifics. The round shape of the bulla and the ventral opening of the meatus represent ancestral conditions in the absence of asymmetric inflation

and the relocation of the external ear in a more dorsal position observed in fossorial and semi-aquatic taxa (see above).

Arboreal rodents have large symmetric bullae. The EAM is short, ventrally located, and anteriorly directed; it has a large opening. As in terrestrial rodents, the position and opening of the EAM reflect a morphology we recognize as typical of above-ground rodents. Although we included gliding rodents in our arboreal category and some gliders (within Sciuridae) have been shown to display enlarged bullae (Lu et al., 2014), this does not explain our finding that arboreal rodents tend to have large auditory bullae. Many of the arboreal rodents we studied that have large auditory bullae are not gliders (e.g., *Erethizon*, *Coendou*, *Capromys*, and *Sphiggurus*) and the arboreal rodents with the smallest bullae are gliders (*Idiurus* and *Glaucomys*). To the best of our knowledge, the bullar sizes of Erethizontidae and Capromyidae have never been thoroughly studied, but a study of octodontoids shows a complex pattern of association between bullar size and ecology (Arnaudo et al., 2020). Together with a study showing that bullar size in Caviomorpha (that did not include erethizontids and capromyids) is variably associated with ecology (Álvarez et al., 2015), our work shows that a rigorous analysis of tympanic bullar morphology across caviomorphs has the potential to shed light on sensory system evolution in rodents. Additionally, future studies expanding on our work should consider bullar morphology in arboreal neotomyines, sigmodontines, and arvicolines (e.g., *Arborimus*) to explore similarities in bullar morphology across rodent clades.

Building upon the association between locomotion and the external bony morphology of the tympanic apparatus, we present locomotory inferences for 24 fossil species. Among those, ten have known locomotory inferences determined by Calede et al. (2019) on the basis of skull morphology or Bertrand et al. (2021) on the basis of endocast morphology. We classify *Capacikala gradatus* as semi-fossorial in this study, the same inference as Calede et al. (2019). We classify *Palaeocastor magnus* as fossorial; this is also the same inference as Calede et al. (2019). Our classification of *Cedromus wilsoni* as arboreal is consistent with prior research, which determined that *Cedromus* was arboreal, fast-moving, had relatively good agility, and improved vision over terrestrial rodents (Bertrand et al., 2017, 2021; Bhagat et al., 2020). *Protosciurus rachelae*, another fossil squirrel, is classified as arboreal by our analyses; a result consistent with prior studies. Its skull has been suggested before to greatly resemble that of modern tree squirrels (Korth & Samuels, 2015) and prior analyses have showed that it was fast-moving (Bhagat et al., 2020) and arboreal (Bertrand et al., 2021). We classify *Altasciurus relictus* (Korth & Tabrum, 2017), an aplodontiid rodent, as arboreal. This result matches with published data. Indeed, prior studies of this taxon have shown similarities in morphology between this taxon and tree squirrels, including *Cedromus*, which we included in our analyses (Hopkins, 2007; Korth & Emry, 1991). A recent analysis of its endocast also inferred an arboreal locomotion for this animal (Bertrand et al., 2021).

Our other inferences are broadly consistent with prior analyses but differ somewhat on degree of fossoriality. Thus, *Entoptychus individens*, *E. wheelerensis*, and *Palaeocastor simplicidens* were all classified as fossorial by Calede et al. (2019), but our analysis classified these three species as semi-fossorial. This is not an unexpected classification due to the similarities between semi-fossorial and fossorial locomotion adaptations. Additionally, other species of *Palaeocastor* have been classified as semi-fossorial based on postcranial morphology (Samuels & Van Valkenburgh, 2008). Taken together, these results suggest that *Entoptychus individens*, *E. wheelerensis*, and *Palaeocastor simplicidens* were not as dramatically adapted to burrowing as some of their relatives (e.g., *P. magnus*). *Meniscomys uhtoffi*, *Tenudomys dakotensis*, and *Bursagnathus aterosseus* were all classified as terrestrial by Calede et al. (2019), but our analysis suggests that they are semi-fossorial. Again, these results are not in fact inconsistent. Calede et al. (2019) determined semi-fossoriality to be the second most likely locomotion for *Meniscomys uhtoffi* and prior research on the ecology of meniscomyine rodents (Hopkins, 2006, 2007) has suggested that *Meniscomys* was a capable burrower. *Bursagnathus* is a perognathine heteromyid (Korth & Samuels, 2015). Modern perognathines, *Chaetodipus* and *Perognathus*, are capable of digging burrows and quadrupedal saltation (Alvarez-Castañeda et al., 2005; Bartholomew & Cary, 1954; Best & Skupski, 1994). *Tenudomys dakotensis*, a stem geomyid, has a ventral morphology of the tympanic bulla, similar to that of *Heteromys gaumeri*, a terrestrial spiny pocket mouse, and a lateral morphology similar to that of *Cynomys ludovicianus*, the black-tailed prairie dog. This latter taxon is a well-known burrower (Hoogland, 1995).

The determination of locomotion based only on tympanic bulla shape enables the study of many species that lack skeletons or even complete skulls in the fossil record. We here provide new locomotory inferences for 14 of these taxa. Among them, *Harrymys irvini* is classified as arboreal by the CVA. *Proharrymys schlaikjeri*, a relative of *Harrymys* (Korth & Branciforte, 2007), has also been classified as arboreal (Calede et al., 2019). In the PCAs, *Harrymys* is found to be most similar in morphology to the semi-fossorial taxa *Lemmus sibiricus* and *Lemmiscus curtatus*. Together, these data suggest that there is some aspect of the skull morphology of Harrymyinae that is similar to arboreal rodents, despite a locomotion that differs from tree-dwelling. Our analyses suggest that it is their inflated bullae and short EAMs with narrow openings. Such morphology is also found in ricochetal taxa like the heteromyid *Dipodomys* (e.g., Bleich, 1977). The presence of *Harrymys* on the edge of the morphospace in our analyses suggests that there are no analogous ecomorphologies in our training sample. Postcranial remains may be necessary to tease apart the locomotory ecology of harrymyines (Calede et al., 2019).

Protosciurus condoni (Thorington et al., 1998) is classified as arboreal. This is consistent with the fact that this tree squirrel has an overall skull morphology which, like other *Protosciurus* species (although not as much as *P. rachelae*), resembles greatly extant arboreal tree squirrels (Korth & Samuels, 2015).

Our analysis classified *Umbogaulus monodon* as fossorial. This is consistent with prior research that has shown that many mylagaulids were fossorial, some highly so (Calede & Hopkins, 2012; Calede & Samuels, 2020; Fagan, 1960; Hopkins, 2007).

We interpret *Schizodontomys amnicolus*, a heteromyid, as semi-fossorial. A different species of *Schizodontomys*, *Schizodontomys*

harkseni, for which there exists postcranial elements, has been qualified as a quadrupedal saltator lacking fossorial specializations (Munthe, 1981). Our classification is consistent with the postcranial morphology. The ecology of *Schizodontomys* resembled that of other quadrupedal semi-fossorial heteromyids like *Chaetodipus* and *Perognathus*. Three of the fossil gophers in our sample have never been included in analyses of locomotion. *Entoptychus planifrons* is classified as semi-fossorial, whereas *Gregorymys curtus*, and an unnamed species of the genus *Entoptychus*, is classified as fossorial. This result is consistent with prior findings of a range of burrowing specializations within Entoptychinae (Calede et al., 2019).

Our analysis is the first to produce a locomotory inference for the family Florentiamyidae. *Florentiamys kingi* is classified as semi-fossorial and *Florentiamys kennethi* as terrestrial. *Florentiamys kingi* displays a reduced bullar expansion and a longer EAM compared to *Florentiamys kennethi*. Morphologically, it appears as if these species occupied different locomotory niches. *Sanctimus falkenbachi* and *Sanctimus stouti*, two other florentiamyids, were classified as terrestrial. Overall, our findings suggest that Florentiamyidae was a predominantly terrestrial family. Quantitative analyses of the postcrania of florentiamyids (Wahlert, 1983; Wood, 1936) will be necessary to assess the diversity of locomotion within the clade.

Our analysis classifies *Mioperognathus willardi* (Korth, 2008) as terrestrial. However, our data suggest that *M. willardi* displays an intermediate ecomorphology. Indeed, our results are equivocal. Our probability that the animal was terrestrial (49%) is only marginally higher than the probability that it was semi-fossorial (46%). *Mioperognathus willardi* is a heteromyid rodent related to modern perognathines, which are semi-fossorial, but it displays a reduced bullar inflation and several other morphological characters considered ancestral for the subfamily (Korth, 2008). *Mioperognathus willardi* may be evidence that a semi-fossorial ecology evolved within perognathines with earlier members of the group being terrestrial.

Paradjidaumo trilophus, a member of the family Eomyidae, is classified as terrestrial. Prior studies of eomyids have confirmed the existence of gliding taxa within the family, but also emphasized the importance of not considering all species within the clade to share the same ecology (Engler & Martin, 2015). In fact, some have been suggested to be tree-dwelling (Daxner-Höck, 2005, 2010) and others demonstrated to be terrestrial (Engler & Martin, 2015). Our work is the first inference of a locomotory mode for a North American species of Eomyidae. Together, with our inference of a terrestrial ecology for the majority of florentiamyids, the terrestrial ecology of *Paradjidaumo* suggests that terrestriality is the ancestral locomotion in Geomorpha.

Most paleontological studies require nearly complete material for locomotory analyses, which is a rare find. Here, we provide a framework that does not require postcrania or even a complete skull to determine locomotion. Indeed, our finding that tympanic bulla morphology is informative of locomotory ecology will enable the inclusion of many more fossil taxa into the study of the evolution of locomotion in rodents. We apply this approach to a specific study system: burrowing rodents of the Oligo-Miocene of North America and their relatives. Our results build upon prior locomotory analyses, supporting their results. In particular, we bring confidence to existing ecological inferences for aplodontiids (Hopkins, 2007; Korth & Emry, 1991; Korth & Samuels, 2015) and mylagaulids (Calede & Hopkins, 2012; Calede & Samuels, 2020; Fagan, 1960; Hopkins, 2007). Our findings also bring complexity to the picture of burrowing evolution within Geomorpha with the existence of several semi-fossorial geomyoids, a diversity of locomotory modes within Entoptychinae, the possible evolution of semi-fossoriality within Perognathinae during the Miocene, and our hypothesis that terrestriality is the ancestral locomotion in Geomorpha.

Our locomotory inferences made from tympanic bulla morphology should be combined with phylogenetic frameworks to reconstruct locomotory evolution. Such an endeavor would be especially valuable in investigating the evolution of burrowing within Geomorpha. For example, the results of our analysis of five species of entoptychine gophers could be combined with prior work (Calede et al., 2019) and existing phylogenetic data (Calede & Rasmussen, 2020) to study the evolution of fossoriality in Oligocene-aged geomyids and, specifically, the number of times that fossoriality evolved within this group. This work can also be undertaken at a broader scale by combining the results for the fourteen species of geomorph rodents we studied with other locomotion data (Calede et al., 2019) and known phylogenetic relationships (Wahlert, 1991). These analyses will enable the rigorous testing of evolutionary ecology hypotheses, including our conjecture that terrestriality is the ancestral locomotion in Geomorpha. Ultimately, this work will enable a more complete analysis of the timing of the evolution of burrowing in Oligo-Miocene rodents of North America.

ACKNOWLEDGEMENTS

Access to specimens was provided by Meg Daly, Bryan Carstens, and Tamaki Yuri (The Ohio State Museum of Biological Diversity), Eric Rickart (Utah Museum of Nature and Science), Elizabeth Wommack, Matthew Carling, and Laura Vietti (University of Wyoming), Jacob Van Veldhuizen and Jaelyn Eberle (University of Colorado at Boulder), John Demboski, Kristen MacKenzie, and Jeff Stephenson (Denver Museum of Nature and Science), Suzanne McLaren and John Wible (Carnegie Museum of Natural History), Roberta Muehlheim (Cleveland Museum of Natural History), Judith Galkin (AMNH), Bill Simpson (FMNH), Samantha Hopkins and Edward Davis (UOMNH), Patricia Holroyd (UCMP), Amanda Milhouse (USNM), Gregory Wilson Mantilla, Ron Eng, and Meredith Rivin (UWBM), Vanessa Rhue and Sam McLeod (LACM), Desui Miao, David Burnham, and Chris Beard (KUVP), and Josh Samuels, Jen Cavin, Chris Schierup, and Keila Bredehoeft (JODA). Photos of UNSM 26686 were shared by Robert Hunt. Josh Samuels shared photos of several fossil specimens. Sam Price and Sam Hopkins shared their time-calibrated phylogenetic tree. Josh Samuels and Sam Hopkins engaged in fruitful conversations. Bryan Carstens provided space at the OSU Museum of Biological Diversity. John Hunter, Andreas Chavez, and Jill Leonard-Pingel provided constructive feedback on an earlier version of this work. Funding was provided by startup funds from the

Ohio State University and a Paleontological Society Norman Newell Early Career Award to JC as well as funds from the Second Year Transformational Program (STEP) at the Ohio State University to ES.

CONFLICT OF INTEREST

The authors have no conflict of interest.

AUTHOR CONTRIBUTIONS

ES and JC designed the project, ES collected the data, JC and ES analyzed the data, and ES and JC drafted and edited the manuscript.

DATA AVAILABILITY STATEMENT

Extant specimen list, centroid size data, hypertrophy data, and PC scores for the training set are available in supplementary tables.

ORCID

Jonathan J. M. Calede https://orcid.org/0000-0002-6905-9719

REFERENCES

Adams, D.C. & Otárola-Castillo, E. (2013) geomorph: an R package for the collection and analysis of geometric morphometric shape data. *Methods in Ecology and Evolution*, 4, 393–399.

Alhajeri, B.H., Hunt, O.J. & Steppan, S.J. (2015) Molecular systematics of gerbils and deomyines (Rodentia: Gerbillinae, Deomyinae) and a test of desert adaptation in the tympanic bulla. *Journal of Zoological Systematics and Evolutionary Research*, 53, 312–330.

Alhajeri, B.H. & Steppan, S.J. (2018) Community structure in ecological assemblages of desert rodents. *Biological Journal of the Linnean Society*, 124, 308–318.

Álvarez, A., Perez, S.I. & Verzi, D.H. (2015) The role of evolutionary integration in the morphological evolution of the skull of caviomorph rodents (Rodentia: Hystricomorpha). *Evolutionary Biology*, 42, 312–327.

Alvarez-Castañeda, S.T., Cortés-Calva, P. & del Rosario Vázquez, M. (2005) Structure and contents of burrows of the pocket mouse (*Chaetodipus rudinoris*) near La Paz, Baja California Sur, Mexico. *Contribuciones Mastozoológicas en Homenaje a Bernardo Villa*, 1, 1–14.

Arnaudo, M.E., Arnal, M. & Ekdale, E.G. (2020) The auditory region of a caviomorph rodent (Hystricognathi) from the early Miocene of Patagonia (South America) and evolutionary considerations. *Journal of Vertebrate Paleontology*, 40(2), e1777557.

Barker, J.M. & Boonstra, R. (2005) Preparing for winter: Divergence in the summer–autumn hematological profiles from representative species of the squirrel family. *Comparative Biochemistry and Physiology Part A: Molecular & Integrative Physiology*, 142, 32–42.

Barnosky, A.D., Hadly, E.A. & Bell, C.J. (2003) Mammalian response to global warming on varied temporal scales. *Journal of Mammalogy*, 84, 354–368.

Bartholomew, G.A. Jr & Cary, G.R. (1954) Locomotion in pocket mice. *Journal of Mammalogy*, 35, 386–392.

Basso, A.P., Sidorkewicj, N.S. & Casanave, E.B. (2017) Methods for estimating the volume of the tympanic bulla in the big hairy armadillo *Chaetophractus villosus* (Mammalia, Xenarthra, Dasypodidae). *International Journal of Morphology*, 35, 128–132.

Becerra, F., Casinos, A. & Vassallo, A.I. (2013) Biting performance and skull biomechanics of a chisel tooth digging rodent (*Ctenomys tuconax*; Caviomorpha; Octodontoidea). *Journal of Experimental Zoology*, 319A, 74–85.

Begall, S. & Burda, H. (2006) Acoustic communication and burrow acoustics are reflected in the ear morphology of the coruro (*Spalacopus cyanus*, Octodontidae), a social fossorial rodent. *Journal of Morphology*, 267, 382–390.

Bertrand, O.C., Amador-Mughal, F. & Silcox, M.T. (2017) Virtual endocast of the early Oligocene *Cedromus wilsoni* (Cedromurinae) and brain evolution in squirrels. *Journal of Anatomy*, 230, 128–151.

Bertrand, O.C., Püschel, H.P., Schwab, J.A., Silcox, M.T. & Brusatte, S.L. (2021) The impact of locomotion on the brain evolution of squirrels and close relatives. *Communications Biology*, 460, 1–15.

Bertrand, O.C., Schillaci, M.A. & Silcox, M.T. (2016) Cranial dimensions as estimators of body mass and locomotor habits in extant and fossil rodents. *Journal of Vertebrate Paleontology*, 36, e1014905.

Best, T.L. & Skupski, M.P. (1994) *Perognathus flavus*. *Mammalian Species*, 471, 1–10.

Bhagat, R., Bertrand, O.C. & Silcox, M.T. (2020) Evolution of arboreality and fossoriality in squirrels and aplodontid rodents: insights from the semicircular canals of fossil rodents. *Journal of Anatomy*, 238, 96–112.

Bivand, R., Rowlingson, B., Diggle, P., Petris, G. & Eglen, S. (2021) *splancs: spatial and space-time pattern analysis*. R package version 2.01-42.

Bleich, V.C. (1977) *Dipodomys stephensi*. *Mammalian Species*, 73, 1–3.

Blois, J.L. & Hadly, E.A. (2009) Mammalian response to Cenozoic climatic change. *Annual Review of Earth and Planetary Sciences*, 37, 181–208.

Brehm, A.M., Tironi, S. & Mortelliti, A. (2020) Effects of trap confinement on personality measurements in two terrestrial rodents. *PLoSONE*, 15, e0221136.

Buffenstein, R. (2000) Ecophysiological responses of subterranean rodents to underground habitats. In: Lacey, E.A., Patton, J.L. & Cameron, G.N. (Eds.) *Life underground: the biology of subterranean rodent*. Chicago: University of Chicago Press, pp. 62–110.

Calede, J.J. (2014) Skeletal morphology of *Palaeocastor peninsulatus* (Rodentia, Castoridae) from the Fort Logan Formation of Montana (early Arikareean): ontogenetic and paleoecological interpretations. *Journal of Mammalian Evolution*, 21, 223–241.

Calede, J.J. & Glusman, J.W. (2017) Geometric morphometric analyses of worn cheek teeth help identify extant and extinct gophers (Rodentia, Geomyidae). *Palaeontology*, 60, 281–307.

Calede, J.J. & Hopkins, S.S.B. (2012) New material of *Alphagaulus pristinus* (Mammalia: Rodentia: Mylagaulidae) from the Deep River Formation (Montana, USA): implications for ecology, ontogeny, and phylogeny. *Journal of Vertebrate Paleontology*, 32, 151–165.

Calede, J.J., Hopkins, S.S.B. & Davis, E.B. (2011) Turnover in burrowing rodents: the roles of competition and habitat change. *Palaeogeography, Palaeoclimatology, Palaeoecology*, 311, 242–255.

Calede, J.J.M. & Rasmussen, D. (2020) New gophers (Rodentia: Geomyidae) from the Cabbage Patch beds of Montana (Renova Formation) and the phylogenetic relationships within Entoptychinae. *Annals of Carnegie Museum*, 86, 107–167.

Calede, J.J.M. & Samuels, J.X. (2020) A new species of *Ceratogaulus* from Nebraska and the evolution of nasal horns in Mylagaulidae (Mammalia, Rodentia, Aplodontioidea). *Journal of Systematic Palaeontology*, 18, 1395–1414.

Calede, J.J.M., Samuels, J.X. & Chen, M. (2019) Locomotory adaptations in entoptychine gophers (Rodentia: Geomyidae) and the mosaic evolution of fossoriality. *Journal of Morphology*, 280, 879–907.

Candela, A.M. & Picasso, M.B.J. (2008) Functional anatomy of the limbs of Erethizontidae (Rodentia, Caviomorpha): indicators of locomotor behavior in Miocene porcupines. *Journal of Morphology*, 269, 552–593.

Carraway, L.N. & Verts, B.J. (1993) *Aplodontia rufa*. *Mammalian Species*, 431, 1–10.

Carrizo, L.V., Tulli, M.J. & Abdala, V. (2014) An ecomorphological analysis of forelimb musculotendinous system in sigmodontine rodents (Rodentia, Cricetidae, Sigmodontinae). *Journal of Mammalogy*, 95, 843–854.

Chaline, J. (1977) Rodents, evolution, and prehistory. *Endeavour*, 1, 44–51.

Chapman, R.C. & Bennett, A.F. (1975) Physiological correlates of burrowing in rodents. *Comparative Biochemistry and Physiology*, 51A, 599–603.

Daxner-Höck, G. (2005) Eomyidae and Gliridae from Rudabánya. *Palaeontographia Italica*, 90, 149–161.

Daxner-Höck, G. (2010) Sciuridae, Gliridae and Eomyidae (Rodentia, Mammalia) from the middle Miocene of St. Stefan in the Gratkorn Basin (Styria, Austria). *Annalen des Naturhistorischen Museums in Wien, Serie A*, 112, 507–536.

Dietl, G.P. & Flessa, K.W. (2011) Conservation paleobiology: putting the dead to work. *Trends in Ecology and Evolution*, 26, 30–37.

Dunn, R.H. & Rasmussen, D.T. (2007) Skeletal morphology and locomotor behavior of *Pseudotomus eugenei* (Rodentia, Paramyinae) from the Uinta Formation, Utah. *Journal of Vertebrate Paleontology*, 27, 987–1006.

Dutt, N.R., Veals, A.M. & Koprowski, J.L. (2020) Resource selection of a montane endemic: sex-specific differences in white-bellied voles (*Microtus longicaudus leucophaeus*). *PLoS One*, 15, e0242104.

Ebensperger, L.A. & Bozinovic, F. (2000) Energetics and burrowing behaviour in the semifossorial degu *Octodon degus* (Rodentia: Octodontidae). *Journal of Zoology*, 252, 179–186.

Elissamburu, A. & de Santis, L. (2011) Forelimb proportions and fossorial adaptations in the scratch-digging rodent *Ctenomys* (Caviomorpha). *Journal of Mammalogy*, 92, 683–689.

Elissamburu, A. & Vizcaíno, S.F. (2004) Limb proportions and adaptations in caviomorph rodents (Rodentia: Caviomorpha). *Journal of Zoology*, 262, 145–159.

Engler, T. & Martin, T. (2015) A partial skeleton of the eomyid *Eomyodon volkeri* Engesser, 1987 (Mammalia: Rodentia) from the late Oligocene Fossil-Lagerstätte of Enspel, Germany. *Palaeobiodiversity and Palaeoenvironments*, 95, 133–147.

Essner, R.L. (2007) Morphology, locomotor behaviour and microhabitat use in North American squirrels. *Journal of Zoology*, 272, 101–109.

Fabre, P.-H., Hautier, L., Dimitrov, D. & Douzery, E.J. (2012) A glimpse on the pattern of rodent diversification: a phylogenetic approach. *BMC Evolutionary Biology*, 12, 88.

Fagan, S.R. (1960) Osteology of *Mylagaulus laevis*, a fossorial rodent from the upper Miocene of Colorado. *University of Kansas Paleontological Contributions*, 9, 1–32.

Famoso, N.A., Davis, E.B., Feranec, R.S., Hopkins, S.S. & Price, S.A. (2016) Are hypsodonty and occlusal enamel complexity evolutionarily correlated in ungulates? *Journal of Mammalian Evolution*, 23, 43–47.

Flynn, L.J., Lindsay, E.H. & Martin, R.A. (2008) Geomorpha. In: Janis, C., Gunnell, G.F. & Uhen, M.D. (Eds.) *Evolution of tertiary mammals of North America*, *2*. Cambridge: Cambridge University Press, pp. 89–125.

Francescoli, G. (2000) Sensory capabilities and communication in subterranean rodents. In: Lacey, E.A., Patton, J.L. & Cameron, G.N. (Eds.) *Life underground: the biology of subterranean rodents*. Chicago: University of Chicago Press, pp. 111–144.

Francescoli, G., Quirici, V. & Sobrero, R. (2012) Patterns of variation in the tympanic bulla of tuco-tucos (Rodentia, Ctenomyidae, Ctenomys). *Acta Theriologica*, 57, 153–163.

Galindo-Leal, C. & Krebs, C.J. (1997) Habitat structure and demographic variability of a habitat specialist: the rock mouse (*Peromyscus difficilis*). *Revista Mexicana de Mastozoologia*, 2, 72–89.

Ginot, S., Hautier, L., Marivaux, L. & Vianey-Liaud, M. (2016) Ecomorphological analysis of the astragalo-calcaneal complex in rodents and inferences of locomotor behaviours in extinct rodent species. *PeerJ*, 4, e2393.

Gobetz, K.E. & Martin, L.D. (2006) Burrows of a gopher-like rodent, possibly *Gregorymys* (Geomyoidea: Geomyidae: Entoptychtinae), from the early Miocene Harrison Formation, Nebraska. *Palaeogeography, Palaeoclimatology, Palaeoecology*, 237, 305–314.

Grafen, A. (1989) The phylogenetic regression. *Philosophical Transactions of the Royal Society, Series B*, 326, 119–157.

Groves, S.L., Peredo, C.M. & Pyenson, N.D. (2021) What are the limits on whale ear bone size? Non-isometric scaling of the cetacean bulla. *PeerJ*, 9, e10882.

Guerrero-Arenas, R., Jiménez-Hidalgo, E. & Genise, J.F. (2020) Burrow systems evince non-solitary geomyid rodents from the Paleogene of southern Mexico. *PLoS One*, 15, e0230040.

Hafner, J.C. & Hafner, M.S. (1988) Heterochrony in rodents. In: McKinney, M.L. (Ed.) *Heterochrony in evolution: a multidisciplinary approach*. New York: Plenum Press, pp. 217–235.

Hastie, T., Tibshirani, R. & Friedman, J.H. (2009) *Elements of statistical learning: data, mining, inference, and prediction*. New York, USA: Springer.

Heffner, R.S. & Heffner, H.E. (1985) Hearing in mammals: the least weasel. *Journal of Mammalogy*, 66, 745–755.

Heffner, R.S. & Heffner, H.E. (1990) Vestigial hearing in a fossorial mammal, the pocket gopher (*Geomys bursarius*). *Hearing Research*, 46, 239–252.

Heffner, R.S. & Heffner, H.E. (1992) Hearing and sound localization in blind mole rats (*Spalax ehrenbergi*). *Hearing Research*, 62, 206–216.

Heffner, R.S., Heffner, H.E., Contos, C. & Kearns, D. (1994) Hearing in prairie dogs: transition between surface and subterranean rodents. *Hearing Research*, 73, 185–189.

Heffner, R.S., Koay, G. & Heffner, H.E. (2001) Audiograms of five species of rodents: implications for the evolution of hearing and the perception of pitch. *Hearing Research*, 157, 138–152.

Hoogland, J. (1995) *The black-tailed prairie dog: social life of a burrowing mammal*. Chicago, Illinois, USA: University of Chicago Press.

Hopkins, S.S.B. (2005) The evolution of fossoriality and the adaptive role of horns in the Mylagaulidae (Mammalia: Rodentia). *Proceedings of the Royal Society B: Biological Sciences*, 272, 1705–1713.

Hopkins, S.S.B. (2006) Morphology of the skull in *Meniscomys* from the John Day Formation of central Oregon. *PaleoBios*, 26, 1–9.

Hopkins, S.S.B. (2007) Causes of lineage decline in the Aplodontidae: testing for the influence of physical and biological change. *Palaeogeography, Palaeoclimatology, Palaeoecology*, 246, 331–353.

Jackson, S.M. (1999) Glide angle in the genus Petaurus and a review of gliding in mammals. *Mammal Review*, 30, 9–30.

Jiménez-Hidalgo, E., Guerrero-Arenas, R. & Smith, K.T. (2018) *Gregorymys veloxikua*, the oldest pocket gopher (Rodentia: Geomyidae), and the early diversification of Geomyoidea. *Journal of Mammalian Evolution*, 25, 427–439.

Kembel, S.W., Cowan, P.D., Helmus, M.R., Cornwell, W.K., Morlon, H., Ackerly, D.D. et al. (2010) Picante: R tools for integrating phylogenies and ecology. *Bioinformatics*, 26, 1463–1464.

Kerber, L. & Sánchez-Villagra, M.R. (2018) Morphology of the middle ear ossicles in the rodent *Perimys* (Neoepiblemidae) and a comprehensive anatomical and morphometric study of the phylogenetic transformations of these structures in caviomorphs. *Journal of Mammalian Evolution*, 26, 407–422.

Kesner, M.H. (1986) The myology of the manus of microtine rodents. *Journal of Zoology*, 210, 1–22.

Kinlaw, A. (1999) A review of burrowing by semi-fossorial vertebrates in arid environments. *Journal of Arid Environments*, 41, 127–145.

Koper, L., Koretsky, I.A. & Rahmat, S.J. (2021) Can you hear me now? A comparative survey of pinniped auditory apparatus morphology. *Zoodiversity*, 55, 63–86.

Korth, W.W. (2008) Two new pocket mice (Mammalia, Rodentia, Heteromyidae) from the Miocene of Nebraska and New Mexico and the early evolution of the subfamily Perognathinae. *Geodiversitas*, 30, 593–609.

Korth, W.W. & Branciforte, C. (2007) Geomyoid rodents (Mammalia) from the Ridgeview Local Fauna, Early-Early Arikareean (Late Oligocene) of western Nebraska. *Annals of Carnegie Museum*, 76, 177–201.

Korth, W.W. & Emry, R.J. (1991) The skull of Cedromus and a review of the Cedromurinae (Rodentia. Sciuridae). *Journal of Paleontology*, 65, 984–994.

Korth, W.W. & Samuels, J.X. (2015) New rodent material from the John Day Formation (Arikareean, Middle Oligocene to Early Miocene) of Oregon. *Annals of Carnegie Museum*, 83, 19–84.

Korth, W.W. & Tabrum, A.R. (2017) A unique rodent fauna from the Whitneyan (Middle Oligocene) of southwestern Montana. *Annals of Carnegie Museum*, 84, 319–340.

Lange, S., Burda, H., Wegner, R.E., Dammann, P., Begall, S. & Kawalika, M. (2006) Living in a "stethoscope": burrow-acoustics promote auditory specializations in subterranean rodents. *Naturwissenschaften*, 94, 134–138.

Langworthy, O.R. & Richter, C.P. (1938) A physiological study of cerebral motor cortex and decerebrate rigidity in the beaver. *Journal of Mammalogy*, 19, 70–77.

Laundré, J.W. (1989) Burrows of least chipmunks in southeastern Idaho. *Northwestern Naturalist*, 70, 18–20.

Lay, D.M. (1972) The anatomy, physiology, functional significance and evolution of specialized hearing organs of gerbilline rodents. *Journal of Morphology*, 138, 41–120.

Lazo-Cancino, D., Rivera, R., Paulsen-Cortez, K., González-Berríos, N., Rodríguez-Gutiérrez, R. & Rodríguez-Serrano, E. (2020) The impacts of climate change on the habitat distribution of the vulnerable Patagonian-Fueguian species *Ctenomys magellanicus* (Rodentia, Ctenomyidae). *Journal of Arid Environments*, 173, 104016.

Lessa, E.P. & Thaeler, C.S. Jr. (1989) A reassessment of morphological specializations for digging in pocket gophers. *Journal of Mammalogy*, 70, 689–700.

Lu, X., Ge, D., Xia, L., Huang, C. & Yang, Q. (2014) Geometric morphometric study of the skull shape diversification in Sciuridae (Mammalia, Rodentia). *Integrative Zoology*, 9, 231–245.

Luna, F. & Antinuchi, C.D. (2007) Energy and distribution in subterranean rodents: sympatry between two species of the genus *Ctenomys*. *Comparative Biochemistry and Physiology*, 147A, 948–954.

Luna, F., Antinuchi, C.D. & Busch, C. (2002) Digging energetics in the South American rodent *Ctenomys talarum* (Rodentia, Ctenomyidae). *Canadian Journal of Zoology*, 80, 2144–2149.

MacLeod, N. (1999) Generalizing and extending the eigenshape method of shape space visualization and analysis. *Paleobiology*, 25, 107–138.

Malizia, A.I. (1998) Population dynamics of the fossorial rodent *Ctenomys talarum* (Rodentia: Octodontidae). *Journal of Zoology*, 244, 545–551.

Mankin, P.C. & Getz, L.L. (1994) Burrow morphology as related to social organization of *Microtus ochrogaster*. *Journal of Mammalogy*, 75, 492–499.

Manger, P.R., Hall, L.S. & Pettigrew, J.D. (1998) The development of the external features of the platypus (*Ornithorhynchus anatinus*). *Philosophical Transactions of the Royal Society of London, Series B: Biological Sciences*, 353, 1115–1125.

Marcy, A.E., Fendorf, S., Patton, J.L. & Hadly, E.A. (2013) Morphological adaptations for digging and climate-impacted soil properties define pocket gopher (*Thomomys* spp.) distributions. *PLoS One*, 8, e64935.

Marcy, A.E., Hadly, E.A., Sherratt, E., Garland, K. & Weisbecker, V. (2016) Getting a head in hard soils: convergent skull evolution and divergent allometric patterns explain shape variation in a highly diverse genus of pocket gophers (*Thomomys*). *BMC Evolutionary Biology*, 16, 207.

Martin, L.D. & Bennett, D.K. (1977) The burrows of the Miocene beaver *Palaeocastor*, western Nebraska, U.S.A. *Palaeogeography, Palaeoclimatology, Palaeoecology*, 22, 173–193.

Mason, M.J. (2001) Middle ear structures in fossorial mammals: a comparison with non-fossorial species. *Journal of Zoology*, 255, 467–486.

Mason, M.J. (2016) Structure and function of the mammalian middle ear. II: inferring function from structure. *Journal of Anatomy*, 228, 300–312.

Mason, M.J., Lai, F.W., Li, J. & Nevo, E. (2010) Middle ear structure and bone conduction in *Spalax*, *Eospalax*, and *Tachyoryctes* mole-rats (Rodentia: Spalacidae). *Journal of Morphology*, 271, 462–472.

Matějů, J. & Kratochvíl, L. (2013) Sexual size dimorphism in ground squirrels (Rodentia: Sciuridae: Marmotini) does not correlate with body size and sociality. *Frontiers in Zoology*, 10, 27.

Merzenich, M.M., Kitzes, L. & Aitkin, L. (1973) Anatomical and physiological evidence for auditory specialization in the mountain beaver (*Aplodontia rufa*). *Brain Research*, 58, 331–344.

Mitteroecker, P., Gunz, P., Windhager, S. & Schaefer, K. (2013) A brief review of shape, form, and allometry in geometric morphometrics, with applications to human facial morphology. *Hystrix*, 24, 59–66.

Momtazi, F., Ghassemzadeh, F. & Zareie, R. (2008) A study of geographical changes of bullae characteristic in genus *Meriones* (Rodentia, Muridae) using outline method. *Iranian Journal of Animal Biosystematics*, 4, 55–62.

Montgomery, W.I. (1980) The use of arboreal runways by the woodland rodents, *Apodemus sylvaticus* (L.), *A. flavicollis* (Melchior) and *Clethrionomys glareolus* (Schreber). *Mammal Review*, 10, 189–195.

Mozaffari, M., Nash, R. & Tucker, A.S. (2021) Anatomy and development of the mammalian external auditory canal: implications for understanding canal disease and deformity. *Frontiers in Cell and Developmental Biology*, 8, 617354.

Munthe, K. (1981) Skeletal morphology and function of the Miocene rodent *Schizodontomys harkseni*. *PaleoBios*, 35, 1–33.

Nevo, E. (1995) Mammalian evolution underground. The ecological genetic-phenetic interfaces. *Acta Theriologica*, 40, 9–31.

Orme, D., Freckleton, R., Thomas, G., Petzoldt, T., Fritz, S. & Nick, I. (2011) Caper: comparative analyses of phylogenetics and evolution in R. R package version 1.0.1.

Ortiz-Caballero, E., Jiménez-Hidalgo, E. & Bravo-Cuevas, V.M. (2020) A new species of the gopher *Gregorymys* (Rodentia, Geomyidae) from the early Oligocene (Arikareean 1) of southern Mexico. *Journal of Paleontology*, 94, 1191–1201.

Paradis, E. & Schliep, K. (2018) Ape 5.0: an environment for modern phylogenetics and evolutionary analyses in R. *Bioinformatics*, 35, 526–528.

Pfaff, C., Martin, T. & Ruf, I. (2015) Bony labyrinth morphometry indicates locomotor adaptations in the squirrel-related clade (Rodentia, Mammalia). *Proceedings of the Royal Society B: Biological Sciences*, 282, 20150744.

Pfeifer, S.R. (1982) Variability in reproductive output and success of *Spermophilus elegans* ground squirrels. *Journal of Mammalogy*, 63, 284–289.

Piras, P., Sansalone, G., Teresi, L., Kotsakis, T., Colangelo, P. & Loy, A. (2012) Testing convergent and parallel adaptations in talpids humeral mechanical performance by means of geometric morphometrics and finite element analysis. *Journal of Morphology*, 273, 696–711.

Pleštilová, L., Hrouzková, E., Burda, H., Meheretu, Y. & Šumbera, R. (2021) Ear morphology in two root-rat species (genus *Tachyoryctes*) differing in the degree of fossoriality. *Journal of Comparative Physiology A*, 207(4), 469–478. https://doi.org/10.1007/s00359-021-01489-z.

Pleštilová, L., Hrouzková, E., Burda, H. & Šumbera, R. (2016) Does the morphology of the ear of the Chinese bamboo rat (*Rhizomys sinensis*) show "subterranean" characteristics? *Journal of Morphology*, 277, 575–584.

Potapova, E.G. (2019) Morphological specificity of the auditory capsule of Sciurid (Sciuridae, Rodentia). *Biology Bulletin*, 46, 730–743.

Price, S.A. & Hopkins, S.S.B. (2015) The macroevolutionary relationship between diet and body mass across mammals. *Biological Journal of the Linnean Society*, 115, 173–184.

R Core Team (2019) *R: a language and environment for statistical computing*. Vienna, Austria: R Foundation for Statistical Computing.

Ransome, D.B. & Sullivan, T.P. (2004) Effects of food and den-site supplementation on populations of *Glaucomys sabrinus* and *Tamiasciurus douglasii*. *Journal of Mammalogy*, 85, 206–215.

Rasmussen, N.L. & Thorington, R.W. (2008) Morphological differentiation among three species of flying squirrels (genus *Hylopetes*) from Southeast Asia. *Journal of Mammalogy*, 89, 1296–1305.

Revell, L.J. (2012) phytools: an R package for phylogenetic comparative biology (and other things). *Methods in Ecology and Evolution*, 3, 217–223.

Revsbech, I.G., Tufts, D.M., Projecto-Garcia, J., Moriyama, H., Weber, R.E., Storz, J.F. & Fago, A. (2013) Hemoglobin function and allosteric regulation in semi-fossorial rodents (family Sciuridae) with different altitudinal ranges. *Journal of Experimental Biology*, 216, 4264–4271.

Rohlf, F.J. (2010) *tpsDig, v2.16*. Stony Brook, New York: Department of Ecology and Evolution, State University of New York at Stony Brook.

Rohlf, F.J. (2013) *tpsUtil, file utility program, v1.58*. Stony Brook, New York: Department of Ecology and Evolution, State University of New York at Stony Brook.

Rohlf, F.J. & Slice, D. (1990) Extensions of the Procrustes method for the optimal superimposition of landmarks. *Systematic Zoology*, 39, 40–59.

Rohlfs, R.V. & Nielsen, R. (2015) Phylogenetic ANOVA: the expression variance and evolution model for quantitative trait evolution. *Systematic Biology*, 64, 695–708.

Rood, J.P. & Test, F.H. (1968) Ecology of the spiny rat, *Heteromys anomalus*, at Rancho Grande, Venezuela. *The American Midland Naturalist*, 79, 89–102.

Russell, R.J. (1968) Evolution and classification of the pocket gophers of the subfamily Geomyinae. *University of Kansas Publications Museum of Natural History*, 16, 473–579.

Rybczynski, N., Ross, E.M., Samuels, J.X. & Korth, W.W. (2010) Re-evaluation of *Sinocastor* (Rodentia: Castoridae) with implications on the origin of modern beavers. *PLoS One*, 5, e13990.

Samuels, J.X. & Hopkins, S.S. (2017) The impacts of Cenozoic climate and habitat changes on small mammal diversity of North America. *Global and Planetary Change*, 149, 36–52.

Samuels, J.X. & Van Valkenburgh, B. (2008) Skeletal indicators of locomotor adaptations in living and extinct rodents. *Journal of Morphology*, 269, 1387–1411.

Samuels, J.X. & Van Valkenburgh, B. (2009) Craniodental adaptations for digging in extinct burrowing beavers. *Journal of Vertebrate Paleontology*, 29, 254–268.

Schleich, C.E. & Vassallo, A.I. (2003) Bullar volume in subterranean and surface-dwelling caviomorph rodents. *Journal of Mammalogy*, 84, 185–189.

Schmitz, L. & Montani, R. (2011) Nocturnality in dinosaurs inferred from scleral ring and orbit morphology. *Science*, 332, 705–708.

Smith, S.M., Angielczyk, K.D., Schmitz, L. & Wang, S.C. (2018) Do bony orbit dimensions predict diel activity pattern in sciurid rodents? *The Anatomical Record*, 301, 1774–1787.

Snyder, D.P. (1982) *Tamias striatus*. *Mammalian Species*, 168, 1–8.

Stein, B.R. (1993) Comparative hind limb morphology in geomyine and thomomyine pocket gophers. *Journal of Mammalogy*, 74, 86–94.

Stein, B.R. (2000) Morphology of subterranean rodents. In: Lacey, E.A., Patton, J.L. & Cameron, G.N. (Eds.) *Life underground: the biology of subterranean rodents*. Chicago: University of Chicago Press, pp. 19–61.

Strauss, R.E. (2010) Discriminating groups of organisms. In: Elewa, A.M.T. (Ed.) *Morphometrics for nonmorphometricians*, Lecture Notes in Earth Sciences. Berlin: Springer, pp. 73–91.

Tabatabaei Yazdi, F., Colangelo, P. & Adriaens, D. (2014) Testing a long-standing hypothesis on the relation between the auditory bulla size and environmental conditions: a case study in two jird species (Muridae: *Meriones libycus* and *M. crassus*). *Mammalia*, 79, 185–200.

Tague, R.G. (2020) Commonality in pelvic anatomy among three fossorial, scratch-digging, mammalian species. *Journal of Mammalian Evolution*, 27, 315–327.

Thorington, R.W., Darrow, K. & Anderson, C.G. (1998) Wing tip anatomy and aerodynamics in flying squirrels. *Journal of Mammalogy*, 79, 245–250.

Turnbull, W.D. (1991) *Protoptychus hatcheri*, Scott, 1895: the Mammalian Faunas of the Washakie Formation, Eocene Age, of Southern Wyoming. Part II. The Adobetown Member, middle division (=Washakie B), Twka/2 (in part). *Fieldiana Geology New Series*, 21, 1–33.

Verde Arregoitia, L.D., Fisher, D.O. & Schweizer, M. (2017) Morphology captures diet and locomotor types in rodents. *Royal Society Open Science*, 4, 160957.

Verzi, D.H. & Olivares, A.I. (2006) Craniomandibular joint in South American burrowing rodents (Ctenomyidae): adaptations and constraints related to a specialized mandibular position in digging. *Journal of Zoology*, 270, 488–501.

Vleck, D. (1979) The energy cost of burrowing by the pocket gopher *Thomomys bottae*. *Physiological Zoology*, 52, 122–136.

Wahlert, J.H. (1983) Relationships of the Florentiamyidae (Rodentia, Geomyoidea) based on cranial and dental morphology. *American Museum Novitates*, 2769, 1–23.

Wahlert, J.H. (1991) The Harrymyinae, a new heteromyid subfamily (Rodentia, Geomorpha), based on cranial and dental morphology of *Harrymys* Munthe, 1988. *American Museum Novitates*, 3013, 1–23.

Wannaprasert, T. (2016) Functional morphology of the ear of the lesser bamboo rat (*Cannomys badius*). *Mammal Study*, 41, 107–117.

Webster, D.B. & Webster, M. (1975) Auditory systems of Heteromyidae: functional morphology and evolution of the middle ear. *Journal of Morphology*, 146, 343–376.

Weisbecker, V. & Schmid, S. (2007) Autopodial skeletal diversity in hystricognath rodents: Functional and phylogenetic aspects. *Mammalian Biology*, 72, 27–44.

Wilkins, K.T., Roberts, J.C., Roorda, C.S. & Hawkins, J.E. (1999) Morphometrics and functional morphology of middle ears of extant pocket gophers (Rodentia: Geomyidae). *Journal of Mammalogy*, 80, 180–198.

Wilkins, K.T. & Woods, C.A. (1983) Modes of mastication in pocket gophers. *Journal of Mammalogy*, 64, 636–641.

Wood, A.E. (1936) A new rodent from the Pliocene of Kansas. *Journal of Paleontology*, 10, 392–394.

Zelditch, M.L., Swiderski, D.L., Sheets, H.D. & Fink, W.L. (2004) *Geometric morphometrics for biologists: a primer*. San Diego: Elsevier Academic Press.

Zherebtsova, O.V. & Potapova, E.G. (2019) Pathways and level of morphological adaptations in modern Diatomyidae and Ctenodactylidae (Rodentia). *Biology Bulletin*, 46, 710–729.

SUPPORTING INFORMATION

Additional supporting information may be found in the online version of the article at the publisher's website.

How to cite this article: Scarpitti, E.A. & Calede, J.J.M. (2021) Ecological correlates of the morphology of the auditory bulla in rodents: Application to the fossil record. *Journal of Anatomy*, 00, 1–22. https://doi.org/10.1111/joa.13579